On Brownian motion with radioactive decay to compute Biot's theory dynamic bulk modulus of gases saturating porous media

Denis Lafarge, Navid Nemati, Stephane Vielpeau

On Brownian motion with radioactive decay to compute Biot's theory dynamic bulk modulus of gases saturating porous media

Denis Lafarge, Navid Nemati, and Stephane Vielpeau

Abstract We present a new simulation method for "accurately" determining the so-called long-wavelength effective dynamic bulk modulus of gases – such as ambient air – saturating porous media of arbitrary microgeometries. The quotation marks at "accurately" remind us, firstly, of the limits of our definition of the effective modulus. These limits are those of the Biot model, often used in noise control applications, which assumes that the geometries remain simple so that the long-wavelength motions of the gas and the solid at the pore scale are those of quasi-incompressible phases. Secondly, they refer to the finite accuracy of the simulation method itself, which converges according to the classical stochastic law in $1/\sqrt{N}$ with N the number of trials. The simulation method is based on the known properties of Brownian motion of diffusing particles which are released in the saturating gas and undergo finite radioactive decay in the bulk and instantaneous absorption at the pore walls. The algorithm is illustrated by showing how the determination of the mean survival times of such particles leads to the calculation of the effective bulk modulus as it is defined in the framework of Biot theory; we also show how it leads to purely geometric constructions to determine a number of parameters such as the static thermal permeability and the static thermal tortuosity. We first validate our radioactive decay Brownian motion simulation technique in the simple case of cylindrical circular pores. The power of this method is further illustrated by rapidly deriving the effective

Denis Lafarge
Laboratoire d'Acoustique de l'Université du Mans, UMR 6613, Avenue O. Messiaen, 72085 Le Mans, denis.lafarge@univ-lemans.fr

Navid Nemati
MSME, Univ Gustave Eiffel, CNRS UMR 8208, Univ Paris Est Crteil, F-77454 Marne-la-Vallee, France, navid.nemati@gmail.com

Stephane Vielpeau
Laboratoire d'Acoustique de l'Université du Mans, UMR 6613, Avenue O. Messiaen, 72085 Le Mans, stephane.vielpeau@univ-lemans.fr

dynamic bulk modulus of ambient saturated air in simple fibrous materials of the type used in noise control applications, supporting in passing the precise frequency-dependent model previously proposed by Lafarge that includes the so-called static thermal permeability, static thermal tortuosity, and thermal characteristic length.

1 Introduction

One of the elements of Biot's linear theory of sound propagation in air-saturated porous materials is the complex effective bulk modulus of air, $K_f(\omega)$, taking into account the thermal exchange between air and solid constituents [1]. This modulus is of concern in many noise control applications when a precise prediction of sound reflection and transmission versus frequency is needed [2]. Let us define it as the factor relating the excess macroscopic pressure[1] P to the mean condensation: $P/K_f(\omega) = \langle\rho\rangle/\rho_0$, where $\langle\rho\rangle$ is

[1] As we assume here that Biot's theory is a relevant description of the actual physics, we assert that the *microscopic* excess-pressure acoustic field in the saturating fluid, (the ambient air, here), p, is to be seen as, very nearly, a spatial pore-scale constant. In other words, in this work there is no important difference to be made between the *microscopic*, p, and averaged *macroscopic*, P, excess-pressure. The near matching between p and P is a consequence of the absence of local resonance, which is also expressed in a related fluid and solid microstructural incompressibility – the former, fluid incompressibility, understood in the sense of the discussion around Eqs. (160-161) in [3], and the latter, in the sense explained later on here, (see sects. 2, 3). Because of these typical incompressibilities in Biot's theory, the pore-scale variations from point to point in the microscopic pressure field p will happen to be very small. Moreover these variations will be entirely removed in the macroscopic average P by defining the latter as: (i) the direct coarse-grained average, $P = \langle p\rangle$, where the averaging $\langle\,\rangle$ is performed in a representative fluid-volume, i.e. the local mean pressure in the air, or else, and in exactly equivalent manner, (ii) the indirect coarse-grained average given by, $\langle p\boldsymbol{v}_i\rangle = P\langle\boldsymbol{v}_i\rangle$, where $\boldsymbol{v}_i$ is the i^{th} component of the microscopic velocity in the fluid, i.e. this time, the "Heaviside-Poynting" or "Umov" averaged pressure (see Refs. [3, 4]) that can also be termed as a "lumped pressure" (see [5]). We assert here that as long as Biot's theory remains relevant, both definitions of P, direct and indirect, are completely equivalent and undistinguishable because of the fluid and solid pore-scale incompressibility. Note that, in what has just been said, we have considered the averaging $\langle\,\rangle = \langle\,\rangle(\boldsymbol{x})$ in a given sample, to be a volume average performed at some central position $\boldsymbol{x}$, (the so-called "Lorentz" point of view in Refs. [4]- [3]). In another poweful point of view, however, that can be used in place of the preceding if *ergodicity* applies, (the so-called "Gibbs" point of view in Refs. [4]- [3]), the averaging $\langle\,\rangle$ is simply viewed as a direct expectation value of the considered quantity, at the position $\boldsymbol{x}$, in an ensemble of realizations of the macroscopic medium. Our definitions of quantities such as the effective bulk modulus, or the thermal permeabilities, will be the same, whether the average $\langle\,\rangle$ is conceived as volume average, ensemble average, or a mix of the two. We note also here that the (macroscopic) volume utilized to perform the macroscopic averages can be replaced by a (macroscopic) surface, see e.g. [6], section 2.

the pore-scale-averaged excess density in the air, and ρ_0 is the air equilibrium density.

Recall that Biot's theory assumes that the acoustic effective wavelengths in the material are large compared to the dimension of averaging volumes. It also assumes, less well known in the literature, a fairly simple geometry in some respects and the absence of resonances, leading to the typical incompressibility that will be discussed, (see footnote 1 and sections 2, 3).

In a low-frequency limit heat exchange between the air and the solid has time to fully establish itself. Then, provided that the porous solid structure is thermally inert enough to act as a thermostat, (i.e. essentially remain at ambient temperature), the air will have to undergo quasi-isothermal expansion and compression [7]. Therefore in this limit $K_f(\omega)$ will tend to the air isothermal bulk modulus K_0, (the atmospheric pressure P_0).

Conversely, in a high-frequency limit, heat exchange does not has time to occur, except in the immediate vicinity of the pore walls, (inside a so-called thermal boundary layer of characteristic thickness $(2\nu'/\omega)^{1/2}$, where $\nu' = \kappa/\rho_0 c_P$ [2] is the thermal diffusivity, κ the thermal conductivity and c_P the specific heat coefficient at constant presssure, of air). The air will undergo adiabatic expansion and compression except in this ever-shrinking vicinity. In this limit $K_f(\omega)$ tends to the adiabatic bulk modulus $K_a = \gamma K_0$, (with $\gamma = c_P/c_V \approx 1.4$, the ratio of specific heat coefficients of air at constant pressure or constant volume). In between, at intermediate frequencies, a smooth relaxation transition is observed, which connects the "relaxed" state, (low-frequency or "static" isothermal limit), to the "frozen" state, (high-frequency adiabatic limit), and is determined by the geometry and dimensions of the pore space and the thermal diffusivity ν' of air.

As will be later discussed in sections 2 and 3, for any specified micro-geometry that respects certain fairly general conditions, the framework of Biot's theory will tend to apply and an effective dynamic bulk modulus of the saturating air will tend to exist, in the sense of the definition sketched above.

It is in principle entirely determined by the solution of a "Fourier" diffusion-controlled problem, which can be stated and solved in the pore space, see [2] Appendix A, or [3] Appendix and the present section 3. In general, because of the complications of the geometries, no closed-form analytic solution can be given and numerical simulations, such as finite differences or finite elements, are required to determine the precise solution.

In practice the geometries present random variations and a given type of material can be best represented by an ensemble of realizations. Thus, the numerical process of obtaining an estimate of $K_f(\omega)$ can become very heavy: first, the local governing equations for the "Fourier" diffusion problem with appropriate boundary conditions have to be solved using numerical techniques such as mentioned; this will be repeated in an ensemble of configurations; and then the results will be configurationally averaged as the

effective bulk modulus will rely averaged fields[2]. As noted by Torquato and Kim in a larger context [8], this can be a wasteful calculation process as there is a significant amount of information that is lost in passing from the local to the averaged fields. To quote them: "such calculations can become exorbitant even when performed on a supercomputer".

In this paper we present a very simple mesh-free algorithm to exactly perform the above operations and compute the effective bulk modulus that appears in Biot's theory, as it is determined by the pore-space geometry and physical parameters of the fluid. The idea of the algorithm, inspired by [8], is not new and was given by one of the authors in [9] with however one blunder in one reasoning, (that just above the incorrect formula [9] (9)). It was then corrected by this author, (see the present Eq. (73)), and, through personal communication applied by other authors to the description of thermal dissipation properties of three-dimensional reconstructed unit cells of aluminum foams saturated by the ambient air [32]. Here we describe precisely the Biot context of the fluid bulk-modulus model, thoroughly justify mathematically (with correction) the calculation procedure [9], give a validation on cylindrical circular tubes and redo the simple illustration cases of Ref. [9].

The paper is organised as follows.

First, we will analyze in section 2 the precise physical position of Biot's theory and clarify what tacit simplifications it makes about microgeometries.

In section 3, we analyze how the notions of dynamic viscous and dynamic thermal tortuosities and permeabilities response functions emerge within Biot's simplifications, and show how the thermal ones determine the effective fluid bulk-modulus.

In the remaining sections we then establish how efficiently these thermal response functions can be calculated, using the *mean survival times of particles undergoing Brownian motion with radioactive decay in the volume and instantaneous absorption at the pore walls*. We obtain in particular purely geometrical procedures to compute some of the purely geometrical parameters embedded in these functions, such as the static thermal permeability, the thermal tortuosity, and higher order quantities.

In section 4 we generalize a set of considerations provided by Lifson and Jackson [10], (elaborating on a method originally due to Pontrjagin, Andronow and Witt [31]), and which lead to the rigorous and simple establishment of the differential equation to which the above survival times obey.

In section 5 we use the results of section 4 and obtain the relevant statistical properties of the Brownian motion paths with radioactive decay, which appear in a construction procedure of ensemble of trajectories proposed by

[2] Here, condensation significantly varies from point to point on the pore scale in the transition regime, where it distributes from isothermal regime values, $b = p/K_0$, at the pore walls, to values tending to the adiabatic regime, $b = p/K_a$, in the central pore region. These need to be ensemble-averaged or volume-averaged, into a so-called macroscopic coarse-grained variable, $B = \langle b \rangle$, to yield an effective bulk modulus in macroscopic relationship, $B = P/K_f(\omega)$.

Torquato and Kim [8]. It expresses finally in the proposed algorithm, that provides an efficient means of obtaining the averaged behaviors and leads directly to the function $K_f(\omega)$ or the Laplace-space representation $K_f(s)$ of the associated operator. This algorithm allows to bypass as much as possible the detailed simulation of the individual Brownian motion paths, and allows to compute configurational macroscopic averages without prior determination of the underlying microscopic fields.

In order to first validate our – pushed to the extreme – synthetic simulation method, we compute in section 6 the effective bulk-modulus for the simple case of parallel cylindrical circular pores, for which we dispose of a well-known closed form analytical result (Zwikker and Kosten's). The power of the method is finally illustrated by deriving the effective dynamic bulk modulus of ambient saturated air in a simple fibrous material of the type used in noise control applications. We show that all the results obtained support the frequency-dependent model proposed long ago by Lafarge [11], [3] Appendix, which includes as geometric parameters besides porosity the so-called static thermal permeability (Lafarge 93, [11]), static thermal tortuosity (Lafarge 93, [11]), and thermal characteristic length (Allard 91, [12]).

Finally, we give conclusions in section 7.

2 Special physical position of Biot's theory and limited scope of the present work

Biot's (1956) classical linear theory [13] is a suitable long-wavelength *semi-empirical model* for describing low-amplitude sound propagation in many different porous elastic solids saturated with compressible viscous fluids, at the macroscopic level where all acoustic variables can be directly coarse-grained. (Their macroscopic values are considered as local direct volume averages realized in the corresponding phase, see footnote 1). Let us immediately emphasize that this model is not completely general in some potentially important aspects, such as the definitions (like the systematic assimilation of macroscopic values to direct volume averages) and the quantities involved. However, we will work here within its framework. This certainly constitutes a kind of special limit or simplification, nonlocal in time, but local in space, of a much more general theory nonlocal in time and space, which has yet to be developed in all its details. As started in [3,4] we know that the construction will not be simple and straightforward. It will have to be the subject of forthcoming theoretical and experimental work.

As we will explain, Biot's theory is essentially based on tacit assumptions made about microstructure, and which lead to the incompressibility of fluid and solid motion on a small scale, i.e. in a representative volume. When these characteristics of fluid and/or solid motion are no longer satisfied at long wavelengths, which may appear for some microgeometries, the macroscopic

model under consideration no longer works and we enter into the realm of the more complicated nonlocal general description mentioned above.

The model was originally developed in the context of geophysical applications where one is concerned with porous media (rocks) saturated by heavy fluids (oil). This model describes a situation in which the fluid and the skeleton, each forming its own infinite cluster connected through the sample, move simultaneously with different macroscopic velocities. With its tacit important assumptions, however, we must realize that this model will not account for all types of poroelastic materials but only for those that respect the incompressibility mentioned above.

In the late 1970s and in the 1980s, important works contributed, if not a fully clarified understanding, at least a better knowledge of Biot's theory. It became established as a relatively general theory of poroelastic fluid-saturated media, which describes the coupled solid and fluid motions, and expresses in coherent manner the inertial, viscous, and elastic interactions between the two phases[3].

It was then used by J.F. Allard & collaborators [17]– [12], [1], and by others, e.g., J.S. Bolton & coll. [22], as the basis for a general description of sound propagation in many common porous acoustic materials saturated by ambient air (polyurethane foams, glass wool, rock wool, etc.) used either singly or in multiple layers with other materials to effectively absorb sound in noise control applications, [1].

In this case it is verified that the same Biot formalism applies with a new feature to be taken into account compared to the original works carried out in the field of geophysics, namely, that the fluid modulus is now an apparent frequency-dependent modulus as it is affected by thermal exchange with the frame.

As described by Johnson in [23] and [6], all the detailed physics of the system microgeometry is hidden in a few parameters; Allard and his collaborators complete the list to describe the frequency-dependent bulk modulus of the fluid.

In the low-frequency limit and in the geophysical context, the important parameters are porosity ϕ, Darcy permeability k_0[4], the static tortuosity α_0, and the abstract Biot-Willis elastic constants P, Q, R, N. In the same low-frequency limit and in the context of air-saturated absorbing materials, the presence of thermal exchange led to the emergence of the so-called static thermal permeability k_0' and static thermal tortuosity α_0', [11], [2], [3].

[3] For example let us mention T.J. Plona and D.L. Johnson establishing the existence of Biot's second compressional wave [14], [15], and R. Burridge and J.B. Keller verifying Biot's equations by applying a special method of homogenization [16] introduced by A. Bensoussan and E. Sanchez-Palencia.

[4] For simplicity of discussion, we express ourselves here as if the material is macroscopically isotropic and the quantities discussed are scalar; the general anisotropic case has been made in section 3. For the heat exchange problem and the bulk modulus of the fluid that interests us here, $K_f(\omega)$, the quantities remain scalar in the general case.

Regarding the elastic constants, P, Q, R and N, they were initially identified through the three *quasi-static* Biot-Willis *Gedanken Experiments* [24]. From the first Gedanken Experiment where the material was subjected to pure shear, N was identified as the shear modulus of the frame itself unaffected by the presence of the viscous saturating fluid, (no restoring shear force arises between the frame and the fluid when the latter is macroscopically sheared). From the other two Gedanken Experiments – one in which a representative volume, jacketed and drained with small capillaries, was subjected to hydrostatic overpressure, and one in which, without a jacket, it was directly subjected to the same hydrostatic overpressure – the remaining macroscopic coefficients P, Q, R are expressed in terms of: ϕ, N, and K_b, K_s, K_f, (see e.g. [23] Eqs. (2.11 a,b,c) or [1] Eqs. (6.18,19,20)), where K_b is the bulk modulus of the frame in vacuo, K_s is the bulk modulus of the elastic solid from which the frame is made, and K_f is the bulk modulus of the saturating fluid itself.

At arbitrary frequencies, Johnson, Koplik and Dashen [6], and Norris [25], (see also [3], Appendix), have described how the parameters k_0 and α_0 combine in a single frequency-dependent dyamic permeability function, $k(\omega)$, or equivalently in a single dynamic tortuosity function, $\alpha(\omega)$, which is directly related to the latter: $\alpha(\omega) \equiv \nu\phi/(-i\omega k(\omega))$, ($\nu = \eta/\rho_0$, with η dynamic viscosity, ν kinematic viscosity). Dynamic tortuosity $\alpha(\omega)$ directly determines the various effective densities that appear in Biot's theory, (ρ_{11}, ρ_{22}, ρ_{12}), and it is a complex frequency-dependent function to account in detail for the inertial-viscous interaction between the solid and the fluid. Explicitly, the densities verify, $\rho_{11} + \rho_{12} = (1-\phi)\rho_s$, $\rho_{22} + \rho_{12} = \phi\rho_0$, and, $\rho_{12} = -(\alpha(\omega) - 1)\,\phi\rho_0$, where ρ_s is the density of the elastic solid on which the frame is built; ρ_{12} describes the inertial-viscous coupling coefficient for the drag that the fluid exerts on the solid, and vice versa by the principle of action and reaction, since both are in different macroscopic motions, one moving and accelerating with respect to the other. Johnson has explained how the functions $\alpha(\omega)$ and $k(\omega)$ are strongly constrained by the condition that the fluid motion at the pore scale is divergence-free to a first approximation in the long wavelength limit of Biot's theory, and as a consequence, has a frequency-dependence that is very well represented in terms of a few geometric parameters, (see again [6] Appendix A and [3] Appendix). Actually, the above relations on the Biot effective densities ρ_{11}, ρ_{12}, ρ_{22}, are obtained on the additional condition that the solid moves entirely as a whole on the pore scale. Thus, we have to say that the latter functions are strongly constrained by the simultaneous conditions of fluid *and* solid incompressibility.

With the work of J.F. Allard & coll. and the consideration of additional loss phenomena associated with, first, internal friction in solids, second, heat exchange between fluids and solids, the theory finally extended its already remarkable predictive power, mentioned in [23]. The theory was found to be particularly useful in noise control applications, [1].

Firstly, it was found that the effect of internal friction in solids can be accounted for by substituting simple frequency-dependent values, (complex amplitude values with so-called small loss angles that are approximately constant), for the coefficients N and K_b in the Biot-Willis expression of the coefficients P, Q, R. Thus, the original Biot-Willis quasi-static Gedanken Experiments are considered to generalize directly in the harmonic regime, now establishing relations bewteen complex amplitude constants.

Secondly, as depicted in the introduction, it has been verified that the thermal exchange between the solid and the fluid leads to an effective, frequency-dependent, bulk modulus of the saturating fluid when the latter is not a liquid, as in the original Biot considerations, but a fluid with a non-negligible coefficient of thermal expansion.

This is the case of gases in general, such as air here. Indeed, real gases have an expansion-compression behavior well described by the perfect gas law, and that means that they have a coefficient of thermal expansion, $\beta_0 \equiv -[\partial\rho/(\rho\partial P)]_{P_0}$, which takes a value very close to $1/T_0$, (T_0, absolute ambient temperature). By the general thermodynamic relation, $\gamma - 1 = T_0\beta_0^2 c_0^2/c_P$, ($c_0 = \sqrt{K_a/\rho_0}$, adiabatic speed of sound), that can be found e.g. in Landau and Lifshitz [26], it means that the factor $\gamma - 1$ deviates significantly from zero, for gases. For liquids, this is not the case because β_0 is very small and, as the thermodynamic relation shows, the deviation is a quadratic effect on β_0. In gases, simple kinetic theory considerations give: $\gamma - 1 = 2/n_d$, which is not small, where n_d is the number of excited degrees of freedom of a typical molecule, (for air, mainly composed of diatomic molecules, $n_d \approx 5$ and $\gamma - 1 \approx 0.4$). In this case, the isothermal K_0 and adiabatic $K_a = \gamma K_0$ bulk moduli differ significantly and there is a frequency dependence of the effective fluid bulk modulus that must be taken into account as already explained in the introduction.

As pointed out by Lafarge, [11], [2], [3], the frequency dependence of the effective fluid bulk modulus is directly obtained through the introduction of the notions of thermal dynamic permeability and thermal dynamic tortuosity, a kind of thermal counterpart of the notions of viscous dynamic permeability and tortuosity. Johnson et al.'s entire analysis of the kind of frequency dependence that appears in these functions [6] translates directly for them, (e.g. [2], Appendix C and [3] Appendix).

Finally, before detailing in the next section (3) how the effective apparent modulus of the fluid $K_f(\omega)$ is defined within the framework of Biot's theory, and then seeing in the following section (4) how it can be calculated, we would like to emphasize once again the limited physical position of Biot's theory and thus the limited scope of our study here.

Biot's theory implicitly constrains the microgeometry (and phase parameters) in such a way that, when focusing on the pore scale, the oscillatory motion of solid and fluid parts can be considered as nearly incompressible phase motion [4], [3]. We may define this feature as the *fundamental incompressibility assumption* at long wavelengths in Biot's theory.

The so-called two space method of homogenization, or double-scale asymptotic homogenization, has in fact a limited scope and limited internal consistency because it automatically leads to this feature at long wavelengths, while we know that there are materials with special microgeometries, not satisfying this incompressibility property. Loosing sight of the semi-empirical nature of Biot's theory, it was sometimes claimed that this theory was rigorously derived from the microstructure by the above-mentioned method of homogenization. However, this was a gross misinterpretation of the character of this homogenization method, which in fact by its process – especially assuming a well-defined pore size – automatically introduced strong simplifications, so strong that they implied the fundamental incompressibility assumption of Biot's theory.

References [4] and [3] explained how a fully general linear theory would be inseparable from the full notions of temporal and spatial dispersion, i.e., non-local temporal and spatial macroscopic responses of the medium. The fully general theory would not satisfy the fundamental assumption of incompressibility and would lead to much richer behavior than Biot theory allows. It remains to be studied in detail. By limiting ourselves here to materials that are well described by Biot theory, we severely limit the scope of our considerations.

Since it is limited to considering solid motions that remain uniform at the pore scale, it is obvious that Biot theory is in principle unable to account for some of the temporal dispersion induced by the non-uniform solid motions at the pore scale (and their reactions to the fluid). Moreover, in combination with the additional divergence-free representation of all fluid displacements at the pore scale, it is equally obvious that it cannot account for spatial dispersion at all. The latter remains completely outside the theoretical framework of Biot's theory.

It is the relatively good satisfaction of the incompressibility of solid and fluid motion at long wavelengths, in a variety of microgeometries, that explains the wide scope and experimental success of Biot's theory. These simplifications in the real propagation problem are expected to hold true and justify Biot's theory, not only when there is a well-defined pore size, but more generally *as long as the complications in the geometries do not lead to the presence of locally resonant structures* [4], [3]. In all these cases, both the long-wavelength spatial dispersion (which is related to the non-uniform or divergent parts of the solid or the fluid motions that occur at the pore scale) and the mentioned additional temporal dispersion (which is also triggered by these motions) are practically absent. This expresses a fact that, compared to the almost uniform (solid) or non-divergent (fluid) motions involved at pore scale in Biot's theory, the actual non-uniform/divergent distributed motions of the solid/fluid at the pore scale are usually of very weak amplitude. Their complete absence in Biot's theory usually does not pose a problem. It is a reasonable simplification.

Therefore, instead of assuming a very well-defined pore size, as is the case with two-scale homogenization, it would be more appropriate to characterize the physical position of Biot theory by recognizing that it corresponds to situations in which one can neglect the long-wavelength spatial dispersion phenomena and a corresponding part of the temporal dispersion, which allows considerable simplifications to be done. We note that the fact that the asymptotic two-scale homogenization method automatically preserves, to a first approximation, the incompressibility of the solid and fluid motion at the pore scale, is an indication that it cannot valuably describe these long-wavelength spatial and specific temporal dispersion phenomena. This failure is also indicative of the inability of the higher order terms in this method to consistently describe the onset of the spatial dispersion corrections that occur at decreasing wavelengths, as well as the part of the temporal dispersion effects associated with this onset. Without detouring through this method as was done in **??**, we can better base our description of the function $K_f(\omega)$ directly and exclusively, on the aforementioned incompressibility of the fluid and solid motions.

In the following, the incompressibility is taken as given. However, the reader should keep in mind that there are scenarios (e.g., with Helmholtz resonators, but not limited to) that would require a complete redefinition of the treatment, which for some materials would lead to a much more general homogenization that will this time account for both spatial and *complete* temporal dispersion.

Since we are making the "incompressible solid and fluid" simplifications here, the factor K_f considered earlier, relating the mean condensation and the excess acoustic pressure in the fluid, will be well-defined and unique, as a complex constant relating complex amplitudes in the harmonic regime, whether the frame oscillations characteristic of Biot theory manifest themselves or not.

This function $K_f(\omega)$, whose form is then independent of the elastic coefficients of the solid phase, will appear in the Biot formalism in the already mentioned Biot-Willis expressions of the elastic Biot coefficients P, Q and R.

Recall that these Biot-Willis expressions were originally derived from quasistatic "jacketed" and "unjacketed" classical *Gedanken Experiments*. It is the incompressible nature of solid and fluid motions at the pore scale that explains that these static thought experiments could be extended to arbitrary frequencies, giving relations having the same form, between complex frequency-dependent values. The Biot-Willis expressions of the elastic Biot coefficients then remained valid in the harmonic regime by using the complex values for the elastic constants arising from the viscoelastic nature of the solid phase and the heat exchange.

This procedure allowed one to express consistently the temporal dispersion that appeared while the basic incompressibility assumption of Biot theory was respected, but would not do in the general case. The above very simple features of the description would be obsolete in the more general framework

of non-local description, and the additional dispersion that lies outside the Biot approach would not necessarily be small.

3 Definition of the dynamic bulk-modulus and related functions

In the class of materials well described by Biot's theory, the actual acoustic vibrations of the poroelastic structures have no effect on the apparent bulk modulus $K_f(\omega)$ of the saturating fluid. Therefore, in what follows and without loss of generality, we can assume that the porous skeleton is sufficiently inert/rigid not to be set in motion. When modeling the effective bulk modulus of air as determined by geometry in the context of Biot's "local theory", this makes it possible to simplify the considerations and calculations in the following in a meaningful way.

The class of materials is limited and we do not allow all types of microgeometries. Since we are working within the framework of Biot's theory, we exclude microgeometries that would include structures such as Helmholtz resonators: Their resonances would trigger the spatial dispersion phenomena (see [3]) that are formally excluded in the Biot description. If we were to perform a general nonlocal homogenization, taking into account all types of microgeometries and thus able to account for the most general spatial and temporal dispersion, we would have to start at the pore scale with the full set of governing coupled equations of sound propagation. In the present case of an inert solid frame, these would be the equations (7.1-7.6) of [3][5].

But for the Biot description we are interested in here, since we implicitly assume incompressibility of the fluid at the pore scale, we must replace this set of coupled equations for inertia, viscosity, elasticity and heat, with a simplified set. This is a string of simpler and unconnected parts, one describing the inertia and viscosity effects, leading to the notion of dynamic viscous permeability and tortuosity, one describing heat exchange, leading to the notion of dynamic thermal permeability and tortuosity, and one expressing only the equation of state from which the relationship between the latter thermal terms and the effective bulk modulus of the fluid is derived. The principle of this simplification has been studied for example in [2], and [3], Appendix. We revisit it in detail here and take the opportunity to comment on what was said earlier about the basic incompressibility assumption of the theory and the relation that this assumption has with the rejection of any description of spatial dispersion and part of temporal dispersion; to our knowledge, these observations have not been made in the given form in the literature before.

[5] In these equations, the zero-velocity boundary condition is set because the porous skeleton is assumed to be motionless; the zero-excess-temperature boundary condition is set because we also assume it to be thermally inert, see [2] Appendix B.3.

First, we will examine the simplified equations, disconnected from the others, that allow us to describe the inertia/viscosity effects.

Let us direct our attention to a finite, coarse-grained spherical region centered at a particular position $\boldsymbol{x}$ within the material and whose radius is chosen large enough to yield meaningful averages, but not so large as to cancel out the actual point-to-point changes that can be meaningfully observed. That is, in addition to a long-wavelength limit that implies a scale separation between the (small) radius of the averaging sphere and the (large) characteristic distance over which the acoustic macroscopic fields vary, we also assume a scale separation between the radius of the averaging sphere and the characteristic distance over which the macroscopic parameters of the material can vary[6]. Under these conditions, the internal structure inside the sphere or averaging ball (b), (with "(b)" for "ball" or "bounded" as its important property is only its limited spatial extent), can be considered as that of a macroscopically homogeneous medium. At the very least, it is representative of the structure of the material at that particular macroscopic position.

Let this solid-fluid averaging ball (b) bounded spherical region have, say, a connected pore space $V_p^{(b)}$ filled by the fluid and a solid-fluid pore wall surface $S_p^{(b)}$. Inherent to Biot's *local* theoretical approach, is the conception that, *the velocity pattern $\boldsymbol{v}(t,\boldsymbol{r})$ in this region of central position $\boldsymbol{x}$, and thus, its macroscopic mean $\langle \boldsymbol{v} \rangle(t,\boldsymbol{x})$ which is the quantity we are interested in, can be seen as a response to the history of macroscopic pressure gradients that have been applied, (at present and past times), at this very position*[7]. Before continuing, and for the purpose of clarity, let us mention that we will distinguish in our mind the spatial derivative operator, say $\boldsymbol{\nabla} = \partial/\partial \boldsymbol{r}$, when it applies to a quantity varying on a microscopic (pore) scale, from the spatial derivative operator with the same notation, $\boldsymbol{\nabla}$, but applied to a coarse-grained quantity such as P or $\langle \boldsymbol{v} \rangle$, varying on a macroscopic scale, and with this time the interpretation, $\boldsymbol{\nabla} = \partial/\partial \boldsymbol{x}$, with $\boldsymbol{x}$ the "central position" of an averaging sphere.

Now, since the actual microscopic air motion in the spherical averaging region satisfies at all times Eq.,

$$\rho_0 \frac{\partial \boldsymbol{v}}{\partial t} = -\boldsymbol{\nabla} p + \eta \nabla^2 \boldsymbol{v} + \left(\frac{\eta}{3} + \zeta\right) \boldsymbol{\nabla}(\boldsymbol{\nabla} \cdot \boldsymbol{v}), \qquad \text{in } V_p^{(b)}, \tag{1}$$

(which is one among the complete set of governing coupling equations mentioned above, η and ζ, first and second viscosities), with boundary conditions:

$$\boldsymbol{v} = \boldsymbol{0}, \qquad \text{on } S_p^{(b)}, \tag{2}$$

---

[6] This leaves open the possibility that the material has small gradients in its macroscopic properties.

[7] This rules out spatial dispersion, which would imply some dependence, as well, on the macroscopic pressure gradients that have been applied at neighboring positions.

and since we, in Biot's theory, apply a divergence-free simplification to the representation of the air motion at the pore scale, we must conclude that we are currently only considering a situation in which the air velocity pattern appearing within the region of the averaging sphere must satisfy, very closely, Eqs. having the following form, which is drastically simplified:

$$\boldsymbol{\nabla} \cdot \boldsymbol{v} = 0, \qquad \text{in } V_p^{(b)}, \tag{3}$$

$$\rho_0 \frac{\partial \boldsymbol{v}}{\partial t} = -\boldsymbol{\nabla} p + \eta \nabla^2 \boldsymbol{v}, \qquad \text{in } V_p^{(b)}, \tag{4}$$

with boundary conditions:

$$\boldsymbol{v} = \boldsymbol{0}, \qquad \text{on } S_p^{(b)}. \tag{5}$$

Because of the lack of suitable boundary conditions on the remaining surfaces bounding in the fluid the averaging sphere, these equations do not define a well-posed problem. A well-defined interpretation/solution of these equations that makes sense as a representation of the velocity field pattern inside the sphere and is consistent with the above view of a velocity pattern that is a response to the time evolution of the applied macroscopic pressure gradients, can, however, be achieved by completing the following.

First, and if necessary[8], we imagine extending in some appropriately defined "uniform way" the domains $V_p^{(b)}$ and $S_p^{(b)}$ in the space outside the sphere, as if the material were macroscopically homogeneous – one can think of a periodic extension, or, a stationary-random extension of the internal structure over all space, generating the domains denoted in what follows $V_p^{(ub)}$ and $S_p^{(ub)}$, with "(ub)" for "unbounded" extension of the structure in the starting ball (b). Note that these regions should be called $V_p^{(ub)}(\boldsymbol{x})$ and $S_p^{(ub)}(\boldsymbol{x})$ because their construction refers to the macroscopic position $\boldsymbol{x}$, where a certain type of local structure of the material is assumed to exist.

Then, we can partition the pressure in this now macroscopically homogeneous *unbounded* region $V_p^{(ub)}$, $S_p^{(ub)}$, into the sum, $p = \pi + P$, of: (i) a given spatially uniformly variable part, P, representing the macroscopic pressure[9], with thus $-\boldsymbol{\nabla} P =$ a pure, time-varying, *spatial constant*, given by the cur-

[8] If the material is macroscopically homogeneous, the extension consists in simply taking for the $V_p^{(ub)}$ and $S_p^{(ub)}$ introduced below the pore space V_p and the pore wall surface S_p of the material itself. If not, we have to perform the indicated extension. Note that the described abstract imaginary construction of a pore space that does not exist reminds us of the introduction of an abtract six-dimensional space in the two-scale homogenization [27], [16].

[9] Pure linear spatial variation is imposed in P as a limit, since, due to the scale separation or long wavelength limit, the macroscopic variation of the pressure in the averaging sphere region – which can be defined by shifting the position of the center of another averaging sphere – tends to be linear.

rent time-varying values of the actual macroscopic pressure gradient at $\boldsymbol{x}$, and (ii) a fluctuating microscopically variable part π with zero mean, ($\langle\pi\rangle = 0$), which is a linear response to the values of the latter gradient at present and past times, and is periodic or stationary-random, respectively, in the case of periodic or stationary-random extension.

We note that the spatial constancy of the macroscopic pressure gradient is a signature of the absence of spatial dispersion in the simplified description above. Since this constancy is direct result of the use of the incompressibility assumption it shows the relationship we have already mentioned, between this assumption and the rejection of spatial dispersion.

With respect to time variations of macroscopic pressure gradients, they can be taken as we wish, (as long as this is compatible with long wavelength considerations), i.e., $-\boldsymbol{\nabla} P = f(t)\boldsymbol{e}(t)$, with arbitrary amplitude function $f(t)$, and arbitrary time-dependent orientation of the unit vector $\boldsymbol{e}$, $\boldsymbol{e}^2 = 1$.

Here, if we allow arbitrary temporal variation, this in no way implies that the full temporal dispersion effect appears in the description. Rather, in this description, the acceptable temporal dispersion effect is very strictly limited. The use of the incompressibility assumption not only excludes the occurrence of spatial dispersion effects, but also it severely limits the temporal dispersion effects: it causes the zeros and singularities of the response functions in the complex frequency plane to lie on the imaginary half-axis instead of the full half-plane allowed by pure causality considerations, see e.g. [6], Appendix A. It follows that these functions are constructed with basis elements that have strictly monotonic behavior on the real frequency axis, see [11], [28], and [3], Appendix. By the way this is explicit in Avellaneda and Torquato's relaxation times representation of the viscous dynamic permeability [29]. This reveals the fact that part of the possible temporal dispersion has been automatically ruled out by the "incompressible solid and fluid" simplification that is inherent to Biot's theory and consistent with the absence of resonance.

Extended in the manner described above, we now have a well-imposed pure inertia/viscosity problem,

$$\boldsymbol{\nabla} \cdot \boldsymbol{v} = 0, \qquad \text{in } V_p^{(ub)}, \tag{6}$$

$$\rho_0 \frac{\partial \boldsymbol{v}}{\partial t} = -\boldsymbol{\nabla}\pi + \eta \nabla^2 \boldsymbol{v} - \boldsymbol{\nabla} P, \qquad \text{in } V_p^{(ub)}, \tag{7}$$

$$\pi : \text{stationary random/ periodic} \qquad \text{in } V_p^{(ub)}, \tag{8}$$

with boundary conditions:

$$\boldsymbol{v} = \boldsymbol{0}, \qquad \text{on } S_p^{(ub)}, \tag{9}$$

defined by geometry, density and first viscosity, and arbitrary values given at different times of the macroscopic pressure gradient at position $\boldsymbol{x}$. It has unique solutions (periodic or stationary random), $\boldsymbol{v}$ and π, in an extended ab-

stract medium, defined by the values $-\boldsymbol{\nabla} P(t', \boldsymbol{x})$ imposed at different times $t' \in [-\infty, t]$, and an interpretation of P as the macroscopic pressure in the starting averaging sphere[10]. Both ways of looking at the macroscopic pressure, $P = \langle p \rangle$, or, $P\langle \boldsymbol{v} \rangle = \langle p\boldsymbol{v} \rangle$, yield exactly the same P value here due to the incompressibility and the periodic or stationary random nature of the $\boldsymbol{v}$ and π fields[11]. Finally, we say that the solution $\boldsymbol{v}$ defined in this way provides an accurate representation of the velocity pattern of the fluid within the averaging sphere originally chosen in the above considerations.

Note that, exactly the same response fields, $\boldsymbol{v}$ and π, will appear in another abstract problem extended as above:

$$\boldsymbol{\nabla} \cdot \boldsymbol{v} = 0, \qquad \text{in } V_p^{(ub)}, \tag{10}$$

$$\rho_0 \frac{\partial \boldsymbol{v}}{\partial t} = -\boldsymbol{\nabla}\pi + \eta \nabla^2 \boldsymbol{v} + \boldsymbol{f}, \qquad \boldsymbol{f} = -\boldsymbol{\nabla} P \qquad \text{in } V_p^{(ub)}, \tag{11}$$

$$\pi : \text{stationary random/ periodic} \qquad \text{in } V_p^{(ub)}, \tag{12}$$

with boundary conditions:

$$\boldsymbol{v} = \boldsymbol{0}, \qquad \text{on } S_p^{(ub)}, \tag{13}$$

and in which the imposed spatial constant $\boldsymbol{f}$, instead of representing a macroscopic pressure gradient, now represents an imposed external, bulk, body force, directly acting in the fluid and given at the different instants by $\boldsymbol{f} = f(t)\boldsymbol{e}(t)$, with $f(t)\boldsymbol{e}(t)$ numerically equal to the previously considered pressure gradient $-\boldsymbol{\nabla} P(t, \boldsymbol{x})$. In this problem, the quantity π, in a way, represents the pressure itself, which appears in the fluid in the given nontrivial microgeometry, in reaction to the imposed, past and present, forces $-\boldsymbol{\nabla} P(t', \boldsymbol{x})$, $t' \in [-\infty, t]$. In the preceding problem, π, in a way, was the local *deviation* to the macroscopic excess pressure. We say "in a way", because, in these mathematical problems, as the fluid is viewed as strictly incompressible which is a pure view of the mind, the quantities apparently playing the role of the real physical excess pressure ($p = P + \pi$ in the first problem, or $p = \pi$ in the second) have only symbolic, not physical, meaning. We cannot expect these abstract purely mathematical quantities to lead to a meaningful

[10] Note that the direct interpretation of "the macroscopic pressure P", $P = \langle p \rangle$, requires π to satisfy $\langle \pi \rangle = 0$. The generally preferable but here completely equivalent interpretation, $P\langle \boldsymbol{v} \rangle = \langle p\boldsymbol{v} \rangle$, requires π to satisfy $\langle \pi \boldsymbol{v} \rangle = \boldsymbol{0}$. These are simultaneously verified here because of the peculiar simplification/assumption of the fluid pore-scale incompressibility. The two simultaneous cancellations can be used to remove in same manner an arbitrary integration constant that otherwise appears in π.

[11] In the general case of arbitrary microgeometry, lying outside the realm of Biot's theory, we will certainly see the direct notion of macroscopic pressure to be replaced by the indirect notion of a macroscopic effective stress H_{ij}, with $-H_{ij}\langle v_j \rangle = \langle p v_i \rangle$; when the fluid motion is almost incompressible we expect H_{ij} to reduce to a diagonal form $-P\delta_{ij}$ with $P = \langle p \rangle$ and $P\langle \boldsymbol{v} \rangle = \langle p\boldsymbol{v} \rangle$, whether the medium is isotropic or not.

representation of the excess physical pressure in the actual physical problem of sound propagation.

In short, within the incompressible fluid simplification here, removing the uniform macroscopic pressure gradient from the microscopic pressure gradient $-\boldsymbol{\nabla} p$ will leave only the microscopically variable periodic or stationary random abstract part $-\boldsymbol{\nabla}\pi$, which also appears with external uniform bulk force acting: exactly the same fluid motion will occur under an imposed macroscopic pressure gradient or under the action of a corresponding external uniform bulk force. The unphysical spatial uniformity of the source terms, related to the divergence-free nature of the motion, is an expression of the fact that the spatial dispersion effects, (intrinsically connected with the spatial variations of source fields), are, by force here, and as we said before, necessarily left entirely outside the description framework. This is why the π, small, abstract pressure variations, will necessarily be *truncated representations* of the physical ones; they will be sufficient for our purpose of accurately representing the velocity pattern but they will not very accurately capture that of the pressure.

With arbitrary time variations of the source terms, (the macroscopic pressure gradient or the external bulk force), the solution is a general convolution of the elementary solution of the Stokes problem considered in [29], (response of the viscous incompressible fluid to a temporal Dirac-delta stirring force, set along a given direction in the stationary random – or periodic – medium). Of course, this solution exhibits the limitations indicated in [6], Appendix A, in that it is constructed with *purely damped* normal modes[12]. By writing the convolution we will learn that there are local "tortuosity" macroscopic operators $\hat{\alpha}_{ij}(\boldsymbol{x})$, or response factors $\alpha_{ij}(t,\boldsymbol{x})$, such that, (with symmetry on the exchange of i and j)

$$\rho_0 \frac{\partial \langle \boldsymbol{v}_i \rangle}{\partial t}(t) = -\hat{\alpha}_{ij}^{-1}(\boldsymbol{x}) \nabla_j P(t) = -\int_{-\infty}^{t} dt' \alpha_{ij}^{-1}(t-t',\boldsymbol{x}) \nabla_j P(t'), \qquad (14)$$

or equivalently, local "permeability" macroscopic operators $\hat{k}_{ij}(\boldsymbol{x})$, or response factors $k_{ij}(t,\boldsymbol{x})$, such that,

$$\phi(\boldsymbol{x}) \langle \boldsymbol{v}_i \rangle(t) = -\frac{\hat{k}_{ij}(\boldsymbol{x})}{\eta} \nabla_j P(t) = -\frac{1}{\eta} \int_{-\infty}^{t} dt' k_{ij}(t-t',\boldsymbol{x}) \nabla_j P(t'). \qquad (15)$$

The above relations are written with $\langle\,\rangle$ performed in the averaging volume of central position $\boldsymbol{x}$ where the values $f(t)\boldsymbol{e}(t)$ of the macroscopic pressure gradient were recorded. Recall that this volume served to construct a representative periodic or stationary random homogeneous medium, so that the

[12] Analogous characteristics and limitations will manifest themselves in the corresponding thermal functions to be introduced next. They express the mentioned fact that within Biot's theory, the temporal dispersion does not appear in its full possible physical generality.

values of the material parameters, porosity ϕ and kernels α_{ij} or k_{ij}, depend on $\boldsymbol{x}$ if the existing starting material has gradients of properties.

In harmonic regime the operators relations (14, 15) become multiplications with the hat quantities becoming the usual frequency-dependent functions, dynamic viscous tortuosity:

$$-i\omega\rho_0\alpha_{ij}(\omega,\boldsymbol{x})\langle\boldsymbol{v}_j\rangle = -\nabla_i P, \tag{16}$$

and dynamic viscous permeability:

$$\phi(\boldsymbol{x})\langle\boldsymbol{v}_i\rangle = -\frac{k_{ij}(\omega,\boldsymbol{x})}{\eta}\nabla_j P. \tag{17}$$

At each position they are computed by solving in the associated unbounded (ub) homogeneous periodic or stationary random medium the following problem:

$$\begin{aligned}
&\boldsymbol{\nabla}\cdot\boldsymbol{v} = 0, && \text{in } V_p^{(ub)}, && \\
&-i\omega\rho_0\boldsymbol{v} = -\boldsymbol{\nabla}\pi + \eta\nabla^2\boldsymbol{v} - \boldsymbol{\nabla}P, && \text{in } V_p^{(ub)}, && (18)\\
&\pi: \quad \textit{stationary random} \quad (\textit{or periodic}) && \text{in } V_p^{(ub)}, && (19)\\
& && && (20)
\end{aligned}$$

with boundary conditions:

$$\boldsymbol{v} = \boldsymbol{0}, \qquad \text{on } S_p^{(ub)}, \tag{21}$$

and $-\boldsymbol{\nabla}P$, a given spatial constant. From the three different unique solutions $\boldsymbol{v}^{(l)}$ associated with the source term $-\boldsymbol{\nabla}P = -\frac{\delta P}{\delta\ell}\boldsymbol{e}^{(l)}$ oriented along the three different mutually orthogonal directions $\boldsymbol{e}^{(l)}$ of the coordinate axis, ($\boldsymbol{e}_i^{(l)} = \delta_{il}$), we get, after averaging in the fluid and using the relations/definitions (16) or (17), the values of the desired functions $k_{ij}(\omega,\boldsymbol{x})$ or $\alpha_{ij}^{-1}(\omega,\boldsymbol{x})$:

$$k_{ij}(\omega,\boldsymbol{x}) = -\frac{\eta\phi(\boldsymbol{x})}{\frac{\delta P}{\delta\ell}}\langle\boldsymbol{v}^{(j)}\rangle\cdot\boldsymbol{e}^{(i)}, \quad \alpha_{ij}^{-1}(\omega,\boldsymbol{x}) = -\frac{(-i\omega\rho_0)}{\frac{\delta P}{\delta\ell}}\langle\boldsymbol{v}^{(j)}\rangle\cdot\boldsymbol{e}^{(i)}. \tag{22}$$

The obtained functions $\alpha_{ij}(\omega,\boldsymbol{x})$ or $k_{ij}(\omega,\boldsymbol{x})$ are automatically symmetric, expressing an Onsager symmetry property, and they are related by:

$$k_{ij}(\omega,\boldsymbol{x}) = \frac{\nu\phi(\boldsymbol{x})}{-i\omega}\alpha_{ij}^{-1}(\omega,\boldsymbol{x}) \tag{23}$$

The frequency-dependent dynamic permeability relation (17) between the macroscopic flow velocity $\phi\langle\boldsymbol{v}\rangle$ and the macroscopic pressure gradient, is referred to as a dynamic regime Darcy's law. The other relation (16) is a dynamic regime Newton's law.

To introduce the analogous notions of dynamic thermal tortuosity and permeability[13], we now proceed, as far as possible, in a somewhat parallel manner. For heat exchange, we are interested in the description of the excess-temperature-pattern τ in air, appearing in the above finite coarse-graining-ball of volume $V_p^{(b)}$ and pore surface $S_p^{(b)}$ centered at $\boldsymbol{x}$. It obeys the following Fourier equation in $V_p^{(b)}$, (which is one among those in the complete set of coupled governing equations mentioned above),

$$\rho_0 c_P \frac{\partial \tau}{\partial t} = \beta_0 T_0 \frac{\partial p}{\partial t} + \kappa \nabla^2 \tau, \qquad \text{in } V_p^{(b)}, \tag{24}$$

with boundary conditions:

$$\tau = 0, \qquad \text{on } S_p^{(b)}. \tag{25}$$

Parallel to what was said earlier for the velocity field, we now claim that it will be inherent in the approach of the *local* theory of Biot to consider *the mean excess temperature pattern* $\langle \tau \rangle(\boldsymbol{x})$*, as a response to the history of macroscopic terms* $\beta_0 T_0 \partial P/\partial t$ *that have been applied (in the present and in the past) at this very position* $\boldsymbol{x}$. To define this response, we first expand, as before, in a suitable "uniform manner" (periodic or stationary random), the domains $V_p^{(b)}$ and $S_p^{(b)}$ so that they encompass the entire space outside the sphere, as if the material were macroscopically homogeneous. Next, we assume that the excess temperature pattern we seek in terms of a periodic or stationary random field is approximately the same as that determined in the following well-posed problem:

$$P = f(t), \qquad \text{in } V_p^{(ub)}, \tag{26}$$

$$\rho_0 c_P \frac{\partial \tau}{\partial t} = \beta_0 T_0 \frac{\partial P}{\partial t} + \kappa \nabla^2 \tau, \qquad \text{in } V_p^{(ub)}, \tag{27}$$

where $f(t)$ is a spatial constant which represents the history of the macroscopic pressure at the central position $\boldsymbol{x}$ of the original averaging ball that served to construct the abstract homogeneous unbounded medium representation ($V_p^{(ub)}$ and $S_p^{(ub)}$), with boundary conditions:

$$\tau = 0, \qquad \text{on } S_p^{(ub)}. \tag{28}$$

[13] Let us note here that, long before the introduction of these ideas by one of us in [11] and [2], T. Levy and E. Sanchez-Palencia in a work using the two-scale homogenization [30], expressed the effective compressibility of the saturating gas in terms of a dynamic thermal function just proportional to our inverse dynamic thermal tortuosity. It was done without noting the parallel existing between suitably defined viscous and thermal functions.

We can justify the way this problem is written as follows. Since P represents the time variations of the macroscopic pressure at the central position $\boldsymbol{x}$ of the original averaging sphere, the equation (27) is reminiscent of the Stokes equation (4) or (11) used to define the velocity pattern after incompressibility was introduced. It should be recalled that the π field did not exactly mimic the deviatoric overpressure, $p - \langle p \rangle$, or the pore-scale distribution of the physical overpressure p around its macroscopic average, but this was not important. The purpose of the plot was to provide an estimate, which could be considered precise in sufficiently simple geometries, of the relationship between the mean velocities and the course of the macroscopic pressure gradients.

By replacing the microscopic variable p with the macroscopic average at the original central sphere position, P, in (27), we again do not attempt to exactly mimic the physical overpressure distribution. In fact, however, the difference between the real overpressure p and the averaged P is of no significance in estimating the relationship between the mean excess temperature in the original sphere and the course of the macroscopic term $\beta_0 T_0 \partial P/\partial t$ with P as the averaged central variable. This is because in the physical problem the deviation $p - P$, where P is this fixed central quantity while p is the physically spatially variable quantity, is by definition averaged towards zero in the original averaging sphere located at the central position $\boldsymbol{x}$. This follows from the definition of P as $P = \langle p \rangle(\boldsymbol{x}, t)$ and from the long wavelengths that ensure symmetric cancellation (within the averaging sphere) of the contributions from the variations associated with the spatial variations of p.

Finally, the problem (24-25) becomes well-posed if it is simplified and extended over the whole space in the way indicated to give (26-27,28). As for the time variations of the uniform excitation P, they can be taken absolutely arbitrarily (as long as they are compatible with long wavelengths), but again, this does not mean that the intervening temporal dispersion will be completely general. For arbitrary time variations, the solution is a convolution of the elementary solution of the Fourier problem considered in [11] (response to a Dirac delta heat source in time). This solution has the constraints given in [2], Appendix C, since it is constructed with *purely damped* normal modes.

By writing the convolution we will learn that there are local macroscopic operators of "thermal tortuosity" $\hat{\alpha}'(\boldsymbol{x})$, associated with response, kernel factors $\alpha'(t, \boldsymbol{x})$, such that,

$$\rho_0 c_P \frac{\partial \langle \tau \rangle}{\partial t}(t) = \hat{\alpha}'^{-1}(\boldsymbol{x}) \beta_0 T_0 \frac{\partial P}{\partial t}(t) = \int_{-\infty}^{t} dt' \alpha'^{-1}(t - t', \boldsymbol{x}) \beta_0 T_0 \frac{\partial P}{\partial t}(t'), \tag{29}$$

or equivalently, local macroscopic operators of "thermal permeability" $\hat{k}'(\boldsymbol{x})$, associated with response, kernel factors $k'(t, \boldsymbol{x})$, such that,

$$\phi\langle\tau\rangle(t) = \frac{\hat{k}'(\boldsymbol{x})}{\kappa}\beta_0 T_0 \frac{\partial P}{\partial t}(t) = \frac{1}{\kappa}\int_{-\infty}^{t} dt' k'(t-t',\boldsymbol{x})\beta_0 T_0 \frac{\partial P}{\partial t}(t'). \tag{30}$$

The above relations are written with $\langle\,\rangle$ performed in the averaging volume of the central position $\boldsymbol{x}$ where the $f(t)$ values of the macroscopic source term $\beta_0 T_0 \partial P/\partial t$ have been recorded. Recall that this volume was used to construct a representative periodic or stationary random homogeneous medium, so that the values of the material parameters, porosity ϕ and kernels α' or k', depend on $\boldsymbol{x}$ if there are gradients in macroscopic properties.

In harmonic regime the operators relations (29, 30) become multiplications with the hat quantities becoming the usual frequency-dependent functions, dynamic thermal tortuosity $\alpha'(\omega,\boldsymbol{x})$:

$$-i\omega\rho_0 c_P \alpha'(\omega,\boldsymbol{x})\langle\tau\rangle = \beta_0 T_0 \frac{\partial P}{\partial t}, \tag{31}$$

and dynamic thermal permeability $k'(\omega,\boldsymbol{x})$:

$$\phi(\boldsymbol{x})\langle\tau\rangle = \frac{k'(\omega,\boldsymbol{x})}{\kappa}\beta_0 T_0 \frac{\partial P}{\partial t}. \tag{32}$$

At each position they are computed by solving in the associated unbounded (ub) homogeneous periodic or stationary random medium the following problem:

$$P = \textit{a given spatial constant} \qquad \text{in } V_p^{(ub)}, \tag{33}$$

$$-i\omega\rho_0 c_P \tau = -i\omega\beta_0 T_0 P + \kappa\nabla^2\tau, \qquad \text{in } V_p^{(ub)}, \tag{34}$$

with boundary conditions:

$$\tau = 0, \qquad \text{on } S_p^{(ub)}. \tag{35}$$

From the unique solution τ, that will automatically be stationary random or periodic, will derive, by averaging in the fluid and by using the relations/definitions (31) and (32), the values of the wanted functions $\alpha'(\omega,\boldsymbol{x})$ or $k'(\omega,\boldsymbol{x})$:

$$k'(\omega,\boldsymbol{x}) = \frac{\kappa\phi(\boldsymbol{x})}{\beta_0 T_0 \partial P/\partial t}\langle\tau\rangle, \quad \alpha'^{-1}(\omega,\boldsymbol{x}) = \frac{(-i\omega\rho_0 c_P)}{\beta_0 T_0 \partial P/\partial t}\langle\tau\rangle, \tag{36}$$

which are related by:

$$k'(\omega,\boldsymbol{x}) = \frac{\nu'\phi(\boldsymbol{x})}{-i\omega}\alpha'^{-1}(\omega,\boldsymbol{x}). \tag{37}$$

The frequency-dependent dynamic thermal permeability relation (32) between the macroscopic excess temperature $\phi\langle\tau\rangle$ and the macroscopic source term, is referred to as a dynamic regime "thermal Darcy's law". The other relation (31) may be referred to as a dynamic regime "thermal Newton's law".

It remains here to explain how these notions of thermal dynamic permeability and tortuosity determine the effective bulk modulus of the air. The link between thermal dynamic permeability/tortuosity and effective bulk modulus has been presented in e.g. [11], [2], or [3]. For completeness we briefly recall here the relation.

As presented in [3], the thermodynamic equation of state of the saturating fluid leads, after linearization, to the following relation between excess pressure, condensation $b \equiv \rho'/\rho_0$ where ρ' is the excess density, and excess temperature:

$$\gamma\chi_0 p = b + \beta_0\tau, \qquad \text{in } V_p^{(b)}, \tag{38}$$

where the notation χ_0 is employed for the adiabatic compressibility $1/K_a$, (setting $\tau = 0$ in (38) the resulting relation $\gamma\chi_0 p = b$ must describe the isothermal excess pressure-condensation relation, so that obviously, $\gamma\chi_0 = 1/K_0$). Taking the average and the time derivative it gives the relation, since $\langle p\rangle = P$,

$$\gamma\chi_0\frac{\partial P}{\partial t} = \frac{\partial\langle b\rangle}{\partial t} + \beta_0\frac{\partial\langle\tau\rangle}{\partial t}. \tag{39}$$

In harmonic regime $e^{-i\omega t}$ and working with the complex amplitudes we can use (31) to express the right-hand side in (39). Using the general thermodynamic identity seen in section 2 and suppressing the common factor $(-i\omega)$ this gives the relation,

$$\chi_0\left[\gamma - \frac{\gamma-1}{\alpha'(\omega,\boldsymbol{x})}\right]P = \langle b\rangle. \tag{40}$$

Therefore in harmonic regime we find a relation having the form,

$$P = K_f(\omega,\boldsymbol{x})\langle b\rangle = \chi_f^{-1}(\omega,\boldsymbol{x})\langle b\rangle, \tag{41}$$

with

$$\begin{aligned} K_f^{-1}(\omega,\boldsymbol{x}) = \chi_f(\omega,\boldsymbol{x}) &= \chi_0\left[\gamma - \frac{\gamma-1}{\alpha'(\omega,\boldsymbol{x})}\right], \\ &= \chi_0\left[\gamma - (\gamma-1)\frac{-i\omega}{\nu'\phi}k'(\omega,\boldsymbol{x})\right]. \end{aligned} \tag{42}$$

It gives the Fourier coefficients of the kernel functions $\chi_f^{-1}(t,\boldsymbol{x})$ or $K_f(t,\boldsymbol{x})$ which appear in the arbitrary time-variable-regime, operator or integral equation,

$$P(t,\boldsymbol{x}) = \hat{\chi}_f^{-1}\langle b\rangle(t,\boldsymbol{x}) = \int_{-\infty}^{t} \chi_f^{-1}(t-t',\boldsymbol{x})\langle b\rangle(t',\boldsymbol{x})dt' \\ = \hat{K}_f\langle b\rangle(t,\boldsymbol{x}) = \int_{-\infty}^{t} K_f(t-t',\boldsymbol{x})\langle b\rangle(t',\boldsymbol{x})dt'. \tag{43}$$

The function $\chi_f(\omega,\boldsymbol{x})$, resp. its inverse $K_f(\omega,\boldsymbol{x})$, represents a local dynamic compressibility, resp. dynamic bulk modulus, of the saturating fluid, that depends on frequency because of the thermal exchanges between fluid and solid.

Finally, we note that it is customary to define a normalized dynamic compressibility $\beta(\omega,\boldsymbol{x})$ such that, in harmonic regime,

$$\chi_0\beta(\omega,\boldsymbol{x})\frac{\partial P}{\partial t} = \frac{\partial\langle b\rangle}{\partial t} = -\boldsymbol{\nabla}\cdot\langle\boldsymbol{v}\rangle. \tag{44}$$

It is given by,

$$\beta(\omega,\boldsymbol{x}) = \frac{\chi_f(\omega,\boldsymbol{x})}{\chi_0} = \gamma - \frac{\gamma-1}{\alpha'(\omega,\boldsymbol{x})}. \tag{45}$$

Note that in (44) we have directly written that, $\partial\langle b\rangle/\partial t = -\boldsymbol{\nabla}\cdot\langle\boldsymbol{v}\rangle$, using the identity $\langle\boldsymbol{\nabla}\cdot\boldsymbol{v}\rangle = \boldsymbol{\nabla}\cdot\langle\boldsymbol{v}\rangle$. We refer the reader to [3] where the explanations are given on how this identity is obtained, (where in the left $\boldsymbol{\nabla} = \partial/\partial\boldsymbol{r}$, and in the right $\boldsymbol{\nabla} = \partial/\partial\boldsymbol{x}$).

4 Generalization of the method of Pontrjagin, Andronow and Witt, in the presence of radioactive decay of diffusing species

As will be seen in section 5 there is a direct proportionality between the distribution of excess temperature field $\tau(\boldsymbol{r})$ in thermal problem defined above (33–35) and the mean survival time $\bar{t}(\boldsymbol{r})$ of a tiny particle released at position $\boldsymbol{r}$, moving and decaying under the combined action of thermal agitation (Brownian motion) and radioactive disintegration, and instantly absorbed by reaching a specified boundary (that of the pore walls). In this section we will first study how to compute the mean survival time $\bar{t}(\boldsymbol{r})$ of the particle with instant absorption at the pore walls.

In a paper on the statistical treatment of dynamic systems, Pontrjagin, Andronow and Witt [31], have discussed a general method, allowing in particular to establish a differential equation for the average time it takes a Brownian motion particle moving under the combined effect of thermal agitation and a stationary field of force, to reach a defined boundary. Focusing on this particular problem, an helpful detailed account of Pontrjagin, Andronow and Witt's general method has been presented by Lifson and Jackson in [10].

Here, closely following Lifson and Jackson's [10] exposition, it is easy to establish a differential equation for the average time it takes for a Brownian motion particle to reach the pore walls, moving under the combined effects of thermal agitation and superimposed radioactive decay of the diffusing species.

In their presentation, Lifson and Jakson [10], as in the general considerations in [31], started with a closed region V bounded by a surface S. Let us substitute for volume V our pore space V_p, occupied by air, and for enclosing surface S, the pore wall surface S_p between air and porous solid. Our pore space V_p is not a closed region but this is not a significant difference. What is important is that this space is only bounded by the surface S_p.

Also, if it happens in our following reasonings that V_p and S_p are not macroscopically homogeneous regions, we will understand to identify them with the homogeneous domains we referred previously by the notations $V_p^{(ub)}(\boldsymbol{x})$, $S_p^{(ub)}(\boldsymbol{x})$, with the dependence $(\boldsymbol{x})$ not indicated, for simplicity. Then, with the substitution of $V_p^{(ub)}$, $S_p^{(ub)}$, for V, S, in [10], only minimal change in the considerations will occur. This is why we take the liberty, in the following, to paraphrase almost completely Lifson and Jakson's exposition, *mutatis mutandis* only what is necessary in the presence of the superimposed radioactive decay of the diffusing particles.

As we will see, varying the radioactive decay time τ_b, from ∞ (no disintegration, low frequency limit), to 0 (instant disintegration, high frequency limit), will allow us to explore the effective bulk-modulus function in its Laplace-Transform variable representation, $K_f(s)$, from $s = 0$, to $s = \infty$, where s is related to ω according to $s = -i\omega$ using the convention $e^{-i\omega t}$.

In [10], the conservative force field, $\boldsymbol{F}(\boldsymbol{r})$, acts on the diffusing species and is required to be finite everywhere in the V_p region. For the sake of generality in this section we retain it, though we need not consider it. We will later (sec 5) set, $\boldsymbol{F}(\boldsymbol{r}) = \boldsymbol{0}$.

We consider Brownian motion particles, moving, in the region V_p, under the combined influence of thermal agitation and the force $\boldsymbol{F}$; the new element compared to [10] is that each diffusing particle undergoes "radioactive decay" with time characteristic τ_b in the volume V_p, i.e., if present (in bulk) at time t the particle has probability $\kappa_b dt = dt/\tau_b$ of being destroyed in the infinitesimal time interval $(t, t + dt)$.

"Disintegration" may be caused by instantaneous chemical reactions, or else, instantaneous interactions in the bulk, resulting in deexcitation of some physical excitation. We define the cumulative probability function $\mathcal{D}(\boldsymbol{r}, t)$, with $\mathcal{D}$ for "Death" or "Decay" or "Disintegration", (replacing the Lifson and Jackson cumulative probability function $\mathcal{W}(\boldsymbol{r}, t)$), as the cumulative probability function that a particle located at point $\boldsymbol{r}$ at time $t = 0$ will reach the bounding surface S_p during the time interval $(0, t)$, or else, will disappear in the bulk V_p without reaching S_p during the same interval.

The "D" Disintegration qualification for this probability is appropriate if any particle touching the surface S_p, or the excitation it carries, is instantly removed; $\mathcal{D}(\boldsymbol{r}, t)$ only differs from $\mathcal{W}(\boldsymbol{r}, t)$ in [10] in that the superimposed

radioactive decay, (of diffusing particles or their excitation), provides an additional spontaneous means of removal, (in bulk).

A number of simple properties previously listed for $\mathcal{W}(\boldsymbol{r},t)$ in [10], still hold for $\mathcal{D}(\boldsymbol{r},t)$.

Evidently, for a point $\boldsymbol{s}$ on the surface S_p, $\mathcal{D}(\boldsymbol{s},t)=1$ for all t. For an interior point we have $\mathcal{D}(\boldsymbol{r},\infty)=1$, while $\mathcal{D}(\boldsymbol{r},0)=0$. A difference with [10] is that the condition,

$$lim_{\tau\to 0}[\mathcal{W}(\boldsymbol{r},\tau)/\tau]=0,$$

now becomes, after accounting for the finite rate of radioactive decay,

$$lim_{\tau\to 0}[\mathcal{D}(\boldsymbol{r},\tau)/\tau]=1/\tau_b=\kappa_b. \tag{46}$$

To see this, recall that $\mathcal{D}(\boldsymbol{r},\tau)$ is the probability that a particle (or its excitation), starting from $\boldsymbol{r}$ at $t=0$, dies before $t=\tau$, either by touching S_p, or by spontaneously decaying in the bulk. So to calculate $\mathcal{D}$, we launch $N\to\infty$ particles at $\boldsymbol{r}$ at $t=0$, and, after a time interval τ, we see N'' paths of particles that have not touched S_p or died in the bulk. The remaining $N'=N-N''$ paths, are dead paths, either stopped in the bulk when particles died spontaneously, or stopped at the boundary S_p where instant decay occurs. Then, $\mathcal{D}(\boldsymbol{r},\tau)=(lim_{N\to\infty})(N'/N)$. When $\tau\to 0$ there is not enough time to reach S_p, so the non-dead path amounts to N'' predicted on the only basis of mass "radioactive" absorption: $N''=N(1-\kappa_b\tau)$; consequently $N'=N\kappa_b\tau$ and $\mathcal{D}=\kappa_b\tau$, as stated in (46).

We can now relate, (as Lifson and Jackson did for probability $\mathcal{W}$), the probability $\mathcal{D}$ at time τ, to its value at the next time $t+\tau$. For this purpose we define the function $\iota(\boldsymbol{r},t,\boldsymbol{\rho})$, such that, $\iota(\boldsymbol{r},t,\boldsymbol{\rho})d\boldsymbol{\rho}$, is the transition probability for a particle, to go from point $\boldsymbol{r}$, in V_p, at time $t=0$, to a volume element $d\boldsymbol{\rho}$ about another point, $\boldsymbol{\rho}$, in V_p, at time t, without having touched the surface S_p during the time interval $(0,t)$. This is not the same as $\upsilon(\boldsymbol{r},t,\boldsymbol{\rho})d\boldsymbol{\rho}$ in [10], because, as our particle now decays in a manner typical of radioactive decay, ι is therefore reduced compared to its counterpart without radioactive decay υ:

$$\iota(\boldsymbol{r},\tau,\boldsymbol{\rho})=e^{-\tau/\tau_b}\upsilon(\boldsymbol{r},\tau,\boldsymbol{\rho}). \tag{47}$$

We may call $\mathcal{L}(\boldsymbol{r},t)\equiv\int_{V_p}\iota(\boldsymbol{r},t,\boldsymbol{\rho})d\boldsymbol{\rho}$ the "Life" expectancy from going to $\boldsymbol{r}$, at $t=0$, to anywhere else in the pore space, at time t. As a particle must be counted as either deceased or living, the function $\iota(\boldsymbol{r},t,\boldsymbol{\rho})$ is normalized in the sense that,

$$\mathcal{L}(\boldsymbol{r},t)\equiv\int_{V_p}\iota(\boldsymbol{r},t,\boldsymbol{\rho})d\boldsymbol{\rho}=1-\mathcal{D}(\boldsymbol{r},t). \tag{48}$$

From (48) and (46) we also note that,

$$(lim_{\tau\to 0})\int_{V_p}\iota(\boldsymbol{r},\tau,\boldsymbol{\rho})d\boldsymbol{\rho}=1-\kappa_b\tau+... \tag{49}$$

It is now clear that the following integral equation holds:

$$\mathcal{D}(\boldsymbol{r},t+\tau)=\mathcal{D}(\boldsymbol{r},\tau)+\int_{V_p}\iota(\boldsymbol{r},\tau,\boldsymbol{\rho})\mathcal{D}(\boldsymbol{\rho},t)d\boldsymbol{\rho}. \tag{50}$$

By the way, the meaning of the above equation is as follows: If a particle has reached the surface S_p during the time interval $(0,t+\tau)$ or has died in the volume V_p during this time interval without touching it, then, either it has reached S_p or died in V_p during the time interval $(0,\tau)$, or else, it gets to the point $\boldsymbol{\rho}$ at time τ without touching the surface S_p or decaying in V_p, and then, reaches from this point the surface S_p or decays in V_p without touching it, in the time interval $(\tau,\tau+t)$[14].

We now recall known results for the successive moments of the ordinary transition probability $\upsilon_0(\boldsymbol{r},t,\boldsymbol{\rho})$ in an infinite medium, which will immediately translate into identical results for the successive moments of $\iota(\boldsymbol{r},t,\boldsymbol{\rho})$.

For Brownian motion without disintegration in a viscous infinite medium in the presence of a field of force, the particle has an average velocity at a point, proportional to the force, i.e., the following limit exists:

$$lim_{\tau\to 0}\frac{\langle\rho_i-r_i\rangle}{\tau}=\frac{F_i}{f}=lim_{\tau\to 0}\tau^{-1}\int_{V_p}(\rho_i-r_i)\,\upsilon_0\,(\boldsymbol{r},\tau,\boldsymbol{\rho})\,d\boldsymbol{\rho}, \tag{51}$$

where f is the hydrodynamic friction coefficient and $\upsilon_0\,(\boldsymbol{r},\tau,\boldsymbol{\rho})$ the transition probability in the infinite medium. Furthermore, the diffusion coefficient $D=kT/f$ is related to the second moment of the displacement, according to,

$$\begin{aligned} lim_{\tau\to 0}\frac{\langle(\rho_i-r_i)(\rho_j-r_j)\rangle}{\tau}&=2D\delta_{ij}\\ =lim_{\tau\to 0}\tau^{-1}\int_{V_p}(\rho_i-r_i)\,(\rho_j-r_j)\,\upsilon_0\,(\boldsymbol{r},\tau,\boldsymbol{\rho})\,d\boldsymbol{\rho}.&\end{aligned} \tag{52}$$

To see this we note that the effect of the force-driven constant drift velocity F_i/f which brings in (ρ_i-r_i) a term $\tau F_i/f$ which superposes to a random, non-driven one, will bring a cross term $\tau^{-1}(F_iF_j)\tau^2/f^2$ which does not contribute in the limit $\tau\to 0$, and two non cross terms that disappear by the absence of direction of the random non-driven motion. Thus no force-driven effect appears in the second moment and the transition probability $\upsilon_0(\boldsymbol{r},t,\boldsymbol{\rho})$ can be replaced by the one without force, Gaussian in each direction, $=\frac{1}{2\pi dDt}e^{-(\boldsymbol{\rho}-\boldsymbol{r})^2/2dDt}$, where d is the dimension. The result then expresses Einstein's translational Brownian motion formula,

[14] Recall that in all reasonings we can imagine replacing the actual V_p, S_p, by the $V_p^{(b)}$, $S_p^{(b)}$, or more precisely, the $V_p^{(ub)}$, $S_p^{(ub)}$.

$\overline{(\rho_i - r_i)(\rho_j - r_j)} = 2D\tau\delta_{ij}$. For all higher moments it can be checked that,

$$\begin{aligned} lim_{\tau\to 0}\tau^{-1}\langle(\rho_i - r_i)^l(\rho_j - r_j)^m(\rho_k - r_k)^n\rangle = 0 \\ = lim_{\tau\to 0}\tau^{-1}\int_{V_p}(\rho_i - r_i)^l(\rho_j - r_j)^m(\rho_k - r_k)^n\,\upsilon_0(\boldsymbol{r},\tau,\boldsymbol{\rho})\,d\boldsymbol{\rho}, \\ (l+m+n) > 2. \end{aligned} \tag{53}$$

Now, in view of the fact that the function $\iota(\boldsymbol{r},t,\boldsymbol{\rho})$ must approach the ordinary (i.e. infinite medium) transition probability as τ approaches to zero, the moments of $\iota(\boldsymbol{r},t,\boldsymbol{\rho})$ must approach the moments of the ordinary transition probability. We then have, from Eqs. (51), (52), and (53),

$$lim_{\tau\to 0}\frac{\langle\rho_i - r_i\rangle}{\tau} = \frac{F_i}{f} = lim_{\tau\to 0}\tau^{-1}\int_{V_p}(\rho_i - r_i)\,\iota(\boldsymbol{r},\tau,\boldsymbol{\rho})\,d\boldsymbol{\rho}, \tag{54a}$$

$$2D\delta_{ij} = lim_{\tau\to 0}\tau^{-1}\int_{V_p}(\rho_i - r_i)(\rho_j - r_j)\,\iota(\boldsymbol{r},\tau,\boldsymbol{\rho})\,d\boldsymbol{\rho}, \tag{54b}$$

$$\begin{aligned} 0 = lim_{\tau\to 0}\tau^{-1}\int_{V_p}(\rho_i - r_i)^l(\rho_j - r_j)^m(\rho_k - r_k)^n\,\iota(\boldsymbol{r},\tau,\boldsymbol{\rho})\,d\boldsymbol{\rho} \\ (l+m+n) > 2. \end{aligned} \tag{54c}$$

We now use the integral equation for $\mathcal{D}(\boldsymbol{r},t)$ [Eq. (50)], to derive a partial differential equation. Expanding $\mathcal{D}(\boldsymbol{\rho},t)$ about the point $\boldsymbol{r}$ we have

$$\begin{aligned} \frac{\partial\mathcal{D}(\boldsymbol{r},t)}{\partial t} &= lim_{\tau\to 0}\tau^{-1}\left[\mathcal{D}(\boldsymbol{r},t+\tau) - \mathcal{D}(\boldsymbol{r},t)\right] \\ &= lim_{\tau\to 0}\tau^{-1}[-\mathcal{D}(\boldsymbol{r},t) + \mathcal{D}(\boldsymbol{r},\tau) \\ &+ \int_{V_p} d\boldsymbol{\rho}\iota(\boldsymbol{r},\tau,\boldsymbol{\rho})[\mathcal{D}(\boldsymbol{r},t) + \sum_i(\rho_i - r_i)\frac{\partial\mathcal{D}}{\partial r_i} \\ &+\frac{1}{2!}\sum_{i,j}(\rho_i - r_i)(\rho_j - r_j)\frac{\partial^2\mathcal{D}}{\partial r_i\partial r_j} + \frac{1}{3!}\sum_{i,j,k}(\rho_i - r_i)(\rho_j - r_j) \\ &\times(\rho_k - r_k)\frac{\partial^3\mathcal{D}}{\partial r_i\partial r_j\partial r_k} + ...]]. \end{aligned} \tag{55}$$

Utilizing the various limiting properties of ι and $\mathcal{D}$ presented in (46), (49), (54a), (54b), (54c), we get a differential equation for the cumulative probability $\mathcal{D}(\boldsymbol{r},t)$ that a particle launched at $\boldsymbol{r}$ in V_p at $t = 0$ vanishes before t, either by touching S_p or decaying in the bulk:

$$\frac{\partial\mathcal{D}}{\partial t} = f^{-1}\boldsymbol{F}\cdot\boldsymbol{\nabla}\mathcal{D} + D\nabla^2\mathcal{D} - \kappa_b\mathcal{D} + \kappa_b. \tag{56}$$

Now observe that the equation, $\mathcal{D}(\boldsymbol{r},t+dt) = \mathcal{D}(\boldsymbol{r},t) + dt\partial\mathcal{D}(\boldsymbol{r},t)/\partial t$, should be interpreted as follows: If a particle starting from $\boldsymbol{r}$ at $t = 0$ vanishes

during the time interval $(0, t+dt)$, (either by reaching S_p or decaying in the bulk V_p), then, either it vanishes during the time interval $(0,t)$, (by reaching S_p or decaying in the bulk V_p), or it is still alive at t, and then, during the time interval $(t, t+dt)$, reaches for the first time S_p or vanishes in the bulk. This shows that $dt\partial\mathcal{D}(\boldsymbol{r},t)/\partial t$ is the probability of a particle to vanish (reach for the first time S_p or vanish in the bulk) during $(t, t+dt)$, when starting from $\boldsymbol{r}$ at time $t=0$. Therefore, the average survival time for a particle is:

$$\bar{t}(\boldsymbol{r}) = \int_0^\infty t \frac{\partial \mathcal{D}}{\partial t}(\boldsymbol{r},t)dt. \tag{57}$$

From this we finally obtain the following desired differential equation satisfied by $\bar{t}(\boldsymbol{r})$:

$$(1/f)\boldsymbol{F}\cdot\boldsymbol{\nabla}\bar{t} + D\nabla^2\bar{t} - \kappa_b\bar{t} = -1, \qquad \text{in } V_p, \tag{58}$$

with boundary condition:

$$\bar{t} = 0, \qquad \text{on } S_p. \tag{59}$$

When the field $\boldsymbol{F}$ is zero one may directly write the solutions for a line, cylinder, and sphere. One has, with $\mu_a \equiv a\sqrt{\kappa_b/D}$,

One dimensional case: length of line $2L$,

$$\bar{t}(x) = \tau_b\left[1 - \frac{cosh(\mu_x)}{cosh(\mu_L)}\right]; \tag{60}$$

Two-dimensional case: radius of cylinder R,

$$\bar{t}(r) = \tau_b\left[1 - \frac{I_0(\mu_r)}{I_0(\mu_R}\right]; \tag{61}$$

Three-dimensional case: radius of sphere R,

$$\bar{t}(r) = \tau_b\left[1 - \frac{\mu_R sinh(\mu_r)}{\mu_r sinh(\mu_R)}\right]. \tag{62}$$

5 Efficient algorithm to compute $\boldsymbol{K_f(\omega)}$ and other functions and intervening parameters

With $\boldsymbol{F}=0$ we can directly compare the average survival time problem (58-59) with the excess temperature pattern problem (33)-(34). Examination of both shows that the following quantities, with the same dimensions, can be put into correspondence:

$$\bar{t} \longleftrightarrow \frac{1}{-i\omega \frac{\beta_0 T_0}{\rho_0 c_P} P} \tau; \tag{63}$$

$$D \longleftrightarrow \frac{\kappa}{\rho_0 c_P} \equiv \nu'; \tag{64}$$

$$\kappa_b \equiv \frac{1}{\tau_b} \longleftrightarrow -i\omega. \tag{65}$$

Therefore, when we have solved the mean survival time problem, we can compute the thermal dynamic permeability by, first, writing the relation (that is deduced by combining (32) with the correspondence (63-65)):

$$k'(\omega) = \phi D \langle \bar{t} \rangle, \tag{66}$$

and next, substituting in the calculations that are made to evaluate the product $D\langle \bar{t} \rangle$, the values $D = \nu'$ and $\kappa_b = -i\omega$ of the coefficients D and κ_b.

Likewise, we can compute the bulk modulus $K_f(\omega)$ by writing the relation (deduced by combining (42 with the correspondence (63-65)):

$$K_f^{-1}(\omega) = K_a^{-1} \left[\gamma - (\gamma - 1) \kappa_b \langle \bar{t} \rangle \right], \tag{67}$$

and substituting the above values of D and κ_b in the expressions obtained for the product $\kappa_b \langle \bar{t} \rangle$. In fact, it means that in the Laplace-variable representation of the kernel $K_f(t)$ of the bulk modulus operator $\hat{K}_f$, (43)[15], we simply have $K_f^{-1}(s) = K_a^{-1} \left[\gamma - (\gamma - 1) \kappa_b \langle \bar{t} \rangle \right]$, with this time, only real positive values $\kappa_b = s$ and $D = \nu'$ in the expressions obtained for the product $\kappa_b \langle \bar{t} \rangle$: The problem of mean survival time is directly relevant to the description of thermal response factors expressed in Laplace representation.

Having established the connection between the mean survival time problem and the thermal problem, let us now show how a simple geometric construction of the Brownian random motion path considered in Torquato & Kim [8], see Figure 1, leads us to a simple geometric algorithm to calculate the mean survival time $\bar{t}$ and its average $\langle \bar{t} \rangle$ over position or over configuration, (see the respective viewpoints of Lorentz and Gibbs, end of footnote 1), and hence also, the thermal functions such as $K_f(\omega)$ that interest us.

For the sake of simplicity of Figure 1 and the discussion here we take our material to be an air-saturated array of parallel fibers with identical radii. Thus only the simulation of diffusion reactions in a medium with static identical circular cylindrical traps in $2D$ needs to be performed; the generalization

[15] By definition the Laplace variable representation is, $K_f(t, \boldsymbol{x}) = \int_{\gamma - i.\infty}^{\gamma + i.\infty} \frac{ds}{2\pi i} e^{st} K_f(s, \boldsymbol{x})$, $K_f(s, \boldsymbol{x}) = \int_0^{\infty} K_f(t, \boldsymbol{x}) e^{-st} dt$, whereas the Fourier representation is, $K_f(t, \boldsymbol{x}) = \int_{-\infty}^{+\infty} \frac{d\omega}{2\pi} K_f(\omega, \boldsymbol{x}) e^{-i\omega t}$, $K_f(\omega, \boldsymbol{x}) = \int_{-\infty}^{\infty} K_f(t, \boldsymbol{x}) e^{i\omega t} dt$; note that in the text here, to lighten the notation we do not make apparent the possible dependance on $\boldsymbol{x}$, e.g. $k'(\omega, \boldsymbol{x}) = \phi(\boldsymbol{x}) D \langle \bar{t} \rangle (\boldsymbol{x})$, that would correspond to interpreting the V_p, S_p, in section 4, as the $V_p^{(ub)}(\boldsymbol{x})$, $S_p^{(ub)}(\boldsymbol{x})$, in section 3.

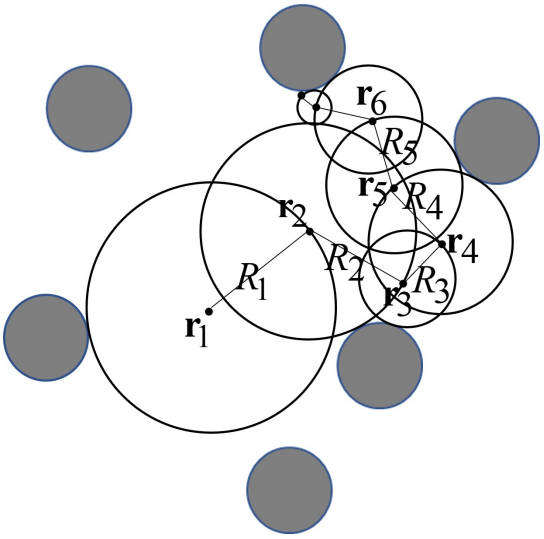

Fig. 1 Schematic representation of the construction of Brownian motion paths $\boldsymbol{r}_1$, $\boldsymbol{r}_2$, ..., $\boldsymbol{r}_n$ with succession of characteristic radii $[R_1, R_2, ..., R_n]$.

to arbitrary microgeometries and $3D$ is obvious and poses no difficulty in principle.

The algorithm to calculate the average survival time $\overline{t}(\boldsymbol{r})$ of random walkers released in one configuration at a given place, or to calculate the average $\langle \overline{t} \rangle$ either viewed as a volume average (in a given configuration) when walkers are released at any place with equal probability, (Lorentz viewpoint), or as an ensemble average when they are released at the same position but the configuration is varied appropriately, (Gibbs viewpoint), is now described.

Let $\boldsymbol{r}_1$ be one arbitrary initial position of the random walker. As observed by Zheng & Chiew [33] and Torquato & Kim [8] the zig-zag motion of the random walker need not be simulated step by step. Instead, one constructs the largest concentric circle/sphere of radius R_1 which does not overlap any solid trap. As the random motion establishes no preference on the directions, the next position $\boldsymbol{r}_1$ of the walker is chosen at random on this circle/sphere.

In this way, Brownian motion paths, $\boldsymbol{r}_1$, $\boldsymbol{r}_2$, ..., $\boldsymbol{r}_n$, are generated, see Figure 1, which can be stopped when $\boldsymbol{r}_n$ is within ϵ of a solid trap, $(R_n < \epsilon)$, which is taken small enough to ensure that, in the problem at hand, the truncation results in insignificant errors.

We now make the necessary modifications to the scheme utilized by the above authors to account for the "radioactive decay" of our random walkers. (These authors utilized the Brownian motion path construction to compute the trapping constant, which is the inverse of our static thermal permeability, whereas we will use it to compute the dynamic thermal permeability or even more directly, the associated relaxation function, see Appendix).

Consider diffusion in one of the circular $2D$ regions of radius R_i defined in the above construction. With R the radius of one such region, we define a hitting probability $p(R)$ that a random walker initially at the center, survives until reaching the boundary. We will start by evaluating this probability, which is unity in the absence of "radioactive decay" (we know that the diffusing walker goes to infinity in an unbounded medium), and smaller than 1 if it exists, since not all particles survive to reach the boundary.

For a random walker starting at the origin O of the region, there are two types of outcomes to the random walk with decay: (i) the decay does not occur before reaching the boundary of radius R, the associated probability is that we want to determine, $p(R)$, and we know that the corresponding mean time, ($\bar{t}_R^{(s)}$, s for surface), to reach R, will be given by the inverse of Einstein's relation, i.e.[16],

$$\bar{t}_R^{(s)} = \frac{R^2}{4D},\ (2D); \quad \bar{t}_R^{(s)} = \frac{R^2}{6D},\ (3D), \tag{68}$$

(ii) the decay occurs before radius R is reached, the associated probability is $1 - p(R)$ and we assume that these aborted random walks are performed in an average time $\bar{t}_R^{(b)}$, (b for bulk). Note that $\bar{t}_\infty^{(b)}$ is the average survival time τ_b of the walker in the infinite medium.

Let $\bar{t}_R$ be the mean survival time of the random walker starting at the origin when being instantly absorbed at the radius R and subject to the radioactive decay. We had it determined in section 4 by Eq. (61) (at $r = 0$) in $2D$, and, Eq. (62) (at $r = 0$) in $3D$:

$$\bar{t}_R = \tau_b \left[1 - \frac{1}{I_0(\mu_R)}\right],\ (2D); \quad \bar{t}_R = \tau_b \left[1 - \frac{\mu_R}{sinh(\mu_R)}\right],\ (3D). \tag{69}$$

But the above two types of outcomes allow us to write it, also, in the following form:

$$\bar{t}_R = [1 - p(R)]\,\bar{t}_R^{(b)} + p(R)\bar{t}_R^{(s)}. \tag{70}$$

To get another relationship between the same, but yet unknown quantities, $p(R)$ and $\bar{t}_R^{(b)}$, let us now imagine that the boundary at radius R is fictitious and drawn in an infinite medium. Let us again follow the particles released in the center O. We know that on average they live the time τ_b. A proportion $1-p(R)$ of them do not reach R and live the average time $\bar{t}_R^{(b)}$. The remaining proportion $p(R)$ reach R and then will later disappear at some instant. The latter particles therefore live first the average time $\bar{t}_R^{(s)}$ to reach R, and then take the additional average time τ_b to disappear. Thus, we have the obvious relation,

[16] Einstein's relation gives the average of the square of the displacement associated with a given diffusion time. The inverse relation gives the average of the diffusion time required to reach a given displacement for the first time. That it has the inverse form of Einstein's relation was demonstrated by Fürth (1917), see G. Klein (1952) [34].

$$\tau_b = [1 - p(R)]\,\bar{t}_R^{(b)} + p(R)\left[\bar{t}_R^{(s)} + \tau_b\right]. \tag{71}$$

Combined with the preceding, it gives, $\tau_b = \bar{t}_R + p(R)\tau_b$, (irrespective of the dimension 2 or 3), that is:

$$\bar{t}_R = \tau_b\,[1 - p(R)]\,. \tag{72}$$

Comparing (72) with (69) we therefore find in the $2D$ and $3D$ cases the following expressions for our hitting probability $p(R)$:

$$p(R) = \frac{1}{I_0(\mu_R)},\ (2D);\quad p(R) = \frac{\mu_R}{sinh(\mu_R)},\ (3D);\quad \mu_R \equiv R\sqrt{\frac{\kappa_b}{D}}. \tag{73}$$

Having determined the probability $p(R)$ – for having survived till crossing for the first time the radius $r = R$, after having started at the centre $r = 0$ – and on the other hand the mean time $\bar{t}_R$ – for crossing for the first time the radius $r = R$ or decaying before touching it, after having started at $r = 0$ – we now can write the following simple expression:

$$\begin{aligned}\bar{t}(\boldsymbol{r}_1, \boldsymbol{r}_2, ..., \boldsymbol{r}_n) = \bar{t}_{R_1} + p(R_1)\bar{t}_{R_2} + p(R_1)p(R_2)\bar{t}_{R_3} \\ +... + p(R_1)...p(R_{n-1})\bar{t}_{R_n},\end{aligned} \tag{74}$$

for the mean time for trapping, associated with the path construction, $\boldsymbol{r}_0, \boldsymbol{r}_1, ..., \boldsymbol{r}_n$, with $R_i = |\boldsymbol{r}_{i+1} - \boldsymbol{r}_i|$. Trapping means here, spontaneously decaying in bulk, or else, instantly decaying by reaching the solid or representative end point of the construction, after having started at $\boldsymbol{r}_1$ at $t = 0$. Finally, by inserting the expression (72) of times $\bar{t}_{R_i}$, a systematic two by two cancellation of all intermediate terms occurs, leaving only the two ends, and giving a result in simpler form:

$$\bar{t}(\boldsymbol{r}_1, \boldsymbol{r}_2, ..., \boldsymbol{r}_n) = \tau_b\,[1 - p(R_1)p(R_2)...p(R_n)]\,. \tag{75}$$

The exact result without truncation will be with $\prod_{i=1}^{\infty} p(R_i)$ for the probability product.

In a given realization of the medium, the final mean survival time $\bar{t}_{\boldsymbol{r}_1}$ at position $\boldsymbol{r}_1$, will be obtained by repeating the path constructions and taking the average over all constructions, of the above mean trapping times:

$$\bar{t}_{\boldsymbol{r}_1} = (lim_{M\to\infty}) \sum \bar{t}(\boldsymbol{r}_0, \boldsymbol{r}_1, ..., \boldsymbol{r}_n)/M, \tag{76}$$

where the sum corresponds to the systematic repetition of the constructions, M is the number of times the constructions are repeated, and the $\boldsymbol{r}_1, ..., \boldsymbol{r}_n$ including the final index value n vary from one construction to another. (In the vectors $[R_1, R_2, ..., R_n]$, only the first value R_1 repeats, all the others, $R_2, ..., R_n$, vary from one construction to another). The exact result without truncation would be, where the overline on the right is the average over the

infinite set of constructions :

$$\bar{t}_{\boldsymbol{r}_1} = \tau_b \left[1 - \overline{\prod_{i=1}^{\infty} p(R_i)} \right]. \tag{77}$$

The excess temperature field at position $\boldsymbol{r}_1$, $\tau(\boldsymbol{r}_1) = -i\omega \frac{\beta_0 T_0}{\rho_0 c_P} P \bar{t}_{\boldsymbol{r}_1}$, (see (64)), will be directly obtained geometrically from the construction of $M \to \infty$ vectors $[R_1, R_2, ..., R_n]$ by applying (74)-(76) and using the expressions (73), (72), of the hitting probability $p(R)$, and survival time $\bar{t}_R$. This determination will correspond to launching M random walkers and making M different constructions, from the same point $\boldsymbol{r_1}$ in one realization, then allowing in the limit $M \to \infty$ the determination of the microscopic field at this point and in this realization. To arrive at the determination of dynamic thermal permeability by averaging $\langle \tau \rangle$, understood as the volume average in a given realization or sample of the medium, it remains to form the volume average which corresponds to the inclusion of all possible initial positions $\boldsymbol{r}_1$ in the representative volume. One way to do so is to take randomly an initial position $\boldsymbol{r_1}$, accept it if it lies in the fluid, and write $\langle \tau \rangle = (lim_{M \to \infty}) \sum \tau(\boldsymbol{r}_1)/M$, where M is the found number of initial positions in the fluid. Thus, this process implies to take a double limit in one sample, the first, of the type of (76), for the determination of the microscopic field at a given position, the second, just above, for its complete variation in the fluid.

Now recall that, as mentioned in the introduction, there is a significant amount of information lost on the way from the local field level to the average. We are now in a position to clarify this important feature, namely that, in order to calculate the average $\langle \tau \rangle$ for the determination of dynamic thermal permeability, it is not necessary to determine the microscopic fields beforehand.

Schematically, two situations should be considered. One (Lorentz) is where the averages are considered as volume averages in a representative volume, as soon as a sample of the medium is given. The other (Gibbs) is where they are considered as ensemble averages, as soon as a representative set of realizations of the medium is given. (Lorentz and Gibbs viewpoints, end of footnote 1). In both cases, we now have the following procedure to calculate the macroscopic average of $\langle \tau \rangle$ which does not require any prior determination of the microscopic field τ.

First consider the case of volume averaging. To calculate the volume average of $\langle \tau \rangle$ we can randomly select an initial position $\boldsymbol{r}_1$ in a representative volume, then perform the construction, $[R_1, R_2, ..., R_n]$, apply our formula (74), and take the average on repetition of this process. Convergence towards the sought macroscopic average will automatically occur as the number of M initial positions $\boldsymbol{r}_1$ increases, without pre-determining the microscopic field $\tau(\boldsymbol{r})$.

In case of ensemble averaging, the initial position $\boldsymbol{r}_1$ is fixed but a new configuration of the traps is considered each time, each time giving rise to a new construction $[R_1, R_2, ..., R_n]$. The sought average is given by the same formulae, for example (75) averaged by repeating the process. Convergence will automatically occur when the number of M constructions increases indefinitely, without any pre-determination in any configuration, of the microscopic field.

In all cases, as we are dealing with stochastic processes, we know that the convergence will be slow, in $1/\sqrt{M}$, with M the used number of constructions.

Before moving on to validation and method examples, it is useful now to restate, further detail, and summarize our findings.

Let us return to the macroscopic average mean life time of a diffusing radioactive species that is directly absorbed in the pore wall. We can consider it either in the Lorentz conception when it is calculated in a single sample by means of constructions derived from random points of a representative fluid volume, or in the Gibbs conception when the point of origin is artificial and invariable and the construction each time is carried out in a new randomly chosen configuration. (Also, mixed conceptions that make partial use of both ways of averaging are possible). By indicating symbolically in all cases, with an overline (which must be interpreted appropriately), the exact way in which the average is performed, one can always designate the mean survival time in question $\bar{t}$ as used in Eq. (77):

$$\bar{t} = \tau_b \left[1 - \overline{\prod_{i=1}^{\infty} p(R_i)} \right]. \tag{78}$$

The important thing is that whatever conception is considered, for the overline it will correspond to a certain vision of the macroscopic medium and a definite procedure to generate the construction $[R_1, R_2, ..., R_n, ...]$ and calculate the average $\overline{\prod_{i=1}^{\infty} p(R_i)}$.

Now recall the correspondence (63-65). There follows immediately from it and the Eqs. (78) and (66) that the dynamic thermal permeability is given by :

$$k'(\omega) = \frac{\nu' \phi}{-i\omega} \left[1 - \overline{\prod_{i=1}^{\infty} p(R_i)} \right]. \tag{79}$$

It is customary to define a thermal relaxation function $\chi'(\omega)$ in such a way that :

$$\frac{1}{\alpha'(\omega)} = 1 - \chi'(\omega). \tag{80}$$

This function is one in the relaxed state, zero in the frozen state. A comparison of this definition (80) with (79) immediately shows that the averaged infinite product $\overline{\prod_{i=1}^{\infty} p(R_i)}$ is nothing but this thermal relaxation function :

$$\chi'(\omega) = \overline{\prod_{i=1}^{\infty} p(R_i)}. \tag{81}$$

Once the relaxation function is conveniently directly determined through the average (81) the other thermal functions derive immediately. The effective bulk modulus, in particular, is given by

$$K_f^{-1}(\omega) = K_a^{-1}\left[1 + (\gamma - 1)\chi'(\omega)\right]. \tag{82}$$

In the low frequency limit, it is a known result [3], [36], that $\alpha'(\omega)$ can be expanded in the following Laurent series:

$$\alpha'(\omega) = \frac{\nu'\phi}{-i\omega k_0'} + \alpha'_0 + \alpha'_1{}^2 \frac{i\omega k_0'}{\nu'\phi} + \alpha'_2{}^3 \left(\frac{i\omega k_0'}{\nu'\phi}\right)^2 + ... \tag{83}$$

where k_0' is the static thermal permeability or inverse trapping constant, α_0' is the static thermal tortuosity, and α_1', α_2', etc., are some higher order purely geometrical dimensionless parameters. Comparing this expansion with the expansions that follow from using Eqs. (81) and (73) with $\mu_R = R\sqrt{\frac{-i\omega}{\nu'}}$, as given by (64-65), and the known small argument expansion of the function I_0 or $sinh$, it is easy to derive explicit geometric expressions for the above geometric parameters. For example in $2D$ for k_0' and α_0' we find :

$$k_0'/\phi = \frac{1}{4}\overline{\sum_{i=1}^{\infty} R_i^2}, \tag{84}$$

and,

$$\frac{k_0'^2 \alpha_0'}{\phi^2} = \overline{\frac{3}{64}\sum_{i=1}^{\infty} R_i^4 + \frac{1}{16}\sum_{i=1}^{\infty}\sum_{j=i}^{\infty} R_i^2 R_j^2}. \tag{85}$$

We let the reader derive higher-order expressions for higher-order geometric parameters.

With respect to the high-frequency limit, we know that we have an expansion in terms of successive powers of the small thermal skin depth, (as long as the pore walls are smooth and are therefore considered as locally flat surfaces at the boundary layer level),

$$\chi'(\omega) = \left(\frac{\nu'}{-i\omega}\right)^{1/2} \frac{2}{\Lambda'} + \frac{\nu'}{-i\omega}\frac{1}{\Sigma'} + ..., \tag{86}$$

with characteristic thermal length Λ', given by, $2/\Lambda' = S_p/V_p$, where S_p and V_p are pore wall surface and pore volume. To our knowledge there is no known general expression for the higher order parameter Σ' which has surface dimensions. In this limit the expression (81) cannot be expanded because for

the first large radii in the product we are in the large argument limit, but for the last very small ones near the pore wall we are in the small argument limit. Nevertheless, given the HF data of the function $\chi'(\omega)$ calculated using (81), we will have the means to estimate the values of the high frequency parameters considering the $\omega \to \infty$ limits, e.g. for Λ' and Σ':

$$\frac{2}{\Lambda'} = lim_{\omega\to\infty} \frac{-i\omega}{\nu'} \overline{\prod_{i=1}^{\infty} p(R_i)}, \tag{87}$$

and,

$$\frac{1}{\Sigma'} = lim_{\omega\to\infty} \frac{-i\omega}{\nu'} \left[\overline{\prod_{i=1}^{\infty} p(R_i)} - \left(\frac{\nu'}{-i\omega} \right)^{1/2} \frac{2}{\Lambda'} \right], \tag{88}$$

where the frequency-dependent complete expressions of the $p(R_i)$ are left.

6 Validation and examples of the method of computation of $K_f(\omega)$ and other functions and intervening parameters

We can now first validate our algorithm 5 by considering a simple case where we have a well-known analytical solution within the Biot framework of the simplifications made. In particular, and for the special case where the material has air-filled pores aligned in identical cylinders, we can choose a situation where the cross-section has a very simple shape, such as a slit, disk or equilateral triangle, so that we can figure out the analytical formula.

To fix our ideas, consider an aligned cylindrical circular pore of radius R. For long wavelength sound propagation along the z-axis of the tube, and coherent with the incompressible simplification in Biot's theory that we mentioned earlier, the set of differential equations governing fluid motion in a single tube can be simplified in the manner done by Zwikker and Kosten [35], which is recalled below. Based on the simplification of the typical fluid incompressibility inherent in Biot's theory, everything happens as if the following governing equations can be combined:

(i) equations determining the velocity pattern :

$$\rho_0 \frac{\partial v}{\partial t} = -\frac{\partial P}{\partial z} + \eta \left(\frac{\partial^2}{\partial x^2} + \frac{\partial^2}{\partial y^2} \right) v, \qquad \textit{(cross-section)}, \tag{89}$$

$$v = 0, \qquad \textit{(pore-wall)}, \tag{90}$$

where $\partial P/\partial z$ is a given spatial constant over the cross-section,

(ii) equations determining the excess temperature pattern :

$$\rho_0 c_P \frac{\partial \tau}{\partial t} = \beta_0 T_0 \frac{\partial P}{\partial t} + \kappa \left(\frac{\partial^2}{\partial x^2} + \frac{\partial^2}{\partial y^2} \right) \tau, \qquad \textit{(cross-section)}, \tag{91}$$

$$\tau = 0, \qquad \textit{(pore-wall)}, \tag{92}$$

where $\beta_0 T_0 \partial P/\partial t$ is again a spatial constant over the cross-section, which will be combined with the following additional relations:

(iii) equation of continuity:

$$\frac{\partial b}{\partial t} + \frac{\partial v}{\partial z} = \frac{1}{\rho_0} \frac{\partial \rho'}{\partial t} + \frac{\partial v}{\partial z} = 0, \qquad \textit{(cross-section)}, \tag{93}$$

and,

(iv) thermodynamic equation of state:

$$\gamma \chi_0 p = b + \beta_0 \tau, \qquad \textit{(cross-section)}. \tag{94}$$

The solution fields v and τ are of the following form:

$$v = \frac{\nu}{-i\omega} \left[-\frac{\partial P}{\eta \partial z} \right] \left[1 - \frac{I_0(\sqrt{\frac{-i\omega}{\nu}} r)}{I_0(\sqrt{\frac{-i\omega}{\nu}} R)} \right] ; \tau = \frac{\nu'}{-i\omega} \left[\beta_0 T_0 \frac{\partial P}{\kappa \partial t} \right] \left[1 - \frac{I_0(\sqrt{\frac{-i\omega}{\nu'}} r)}{I_0(\sqrt{\frac{-i\omega}{\nu'}} R)} \right]. \tag{95}$$

For the case of other cross-sectional shapes of cylindrical tubes, the same differential equations and boundary conditions will apply, but must be solved taking into account the particular shape of the geometry.

With $\langle\,\rangle$ denoting the average at the cross section of the tube, we can define macroscopic variables such as average axial velocity $\langle v \rangle$, average overpressure $P = \langle p \rangle$, average over-density $\langle \rho' \rangle$, or average condensation $B = \langle b \rangle = \langle \rho' \rangle / \rho_0$.

Therefore, comparing the above-mentioned governing equations (possibly written in the general cylindrical case) with those discussed in sect. 3, we see that in the harmonic regime we have, at the macroscopic, averaged level, a viscous, dynamic Darcy law, stating that :

$$\langle v \rangle = -\frac{k(\omega)}{\eta} \frac{\partial P}{\partial z}, \tag{96}$$

where $k(\omega)$ can be directly computed by using this definition and the average at the cross-section, of the harmonic regime solution $v(x, y)$. For the cylindrical circular tube, $v(x, y) = v(r)$ is given by (95), and a straightforward integration shows that :

$$k(\omega) = \frac{\nu}{-i\omega} \left[1 - 2 \frac{I_1 \left(\sqrt{\frac{-i\omega}{\nu}} R \right)}{\left(\sqrt{\frac{-i\omega}{\nu}} R \right) I_0 \left(\sqrt{\frac{-i\omega}{\nu}} R \right)} \right]. \tag{97}$$

In general it is convenient to express the dynamic viscous tortuosity in terms of its high-frequency limit, α_∞, and a viscous relaxation-function, $\chi(\omega)$, taking a value of 1 when the viscous effects are in a relaxed state, (vortical motions originating from the pore walls having time to fully penetrate the fluid during the cycle time), and a value of 0 when they are in a frozen state, (vortical motions having no time to penetrate the fluid during the cycle time):

$$\frac{1}{\alpha(\omega)} = \frac{1}{\alpha_\infty}\left[1 - \chi(\omega)\right]. \tag{98}$$

For all cylindrical tubes α_∞ is equal to 1. The non-trivial expression in the above brackets (97) is just the above relaxation-function $\chi(\omega)$ for the cylindrical circular case.

In the same way, the comparison of the above-mentioned equations with those of sect. 3, also leads us to the analogous thermal and dynamic "Darcy" law, which states that :

$$\langle \tau \rangle = \frac{k'(\omega)}{\kappa} \beta_0 T_0 \frac{\partial P}{\partial t}, \tag{99}$$

where $k'(\omega)$ can be directly computed by using this definition and the average at the cross-section, of the harmonic regime solution $\tau(x, y)$. For the cylindrical circular tube, $\tau(x, y) = \tau(r)$ is given by (95), and the integration shows that :

$$k'(\omega) = \frac{\nu'}{-i\omega}\left[1 - 2\frac{I_1\left(\sqrt{\frac{-i\omega}{\nu'}}R\right)}{\left(\sqrt{\frac{-i\omega}{\nu'}}R\right) I_0\left(\sqrt{\frac{-i\omega}{\nu'}}R\right)}\right]. \tag{100}$$

The non-trivial function, in the bracket, is just the thermal relaxation function for the cylindrical circular tube :

$$\chi'_{circ}(\omega) = 2\frac{I_1\left(\sqrt{\frac{-i\omega}{\nu'}}R\right)}{\left(\sqrt{\frac{-i\omega}{\nu'}}R\right) I_0\left(\sqrt{\frac{-i\omega}{\nu'}}R\right)}. \tag{101}$$

In general, obviously, for the cylindrical tubes more generally the viscous and thermal problems are essentially the same and the frequency-dependences are direcly transformed by the relations, $\chi'(\omega) = \chi(\omega Pr)$, or, $k(\omega) = k'(\omega/\,\mathrm{Pr})$, $\alpha(\omega) = \alpha'(\omega/\,\mathrm{Pr})$, coming from the identity, $\mathrm{Pr} = \nu/\nu'$, where Pr is the Prandtl number.

Finally, to validate our simulation technique in the case of a circular tube, we only need to check, in essence, that, when we randomly launch the initial position of a random walker inside a disk of radius R, then construct and average the probability product over a large number of trials, we find:

$$\overline{\prod_{i=1}^{\infty} p(R_i)} = \chi'_{circ}(\omega). \tag{102}$$

In Figure 2 we present an Argand plot of this relaxation function, as given by the theoretical Eq. (101), and as estimated with $N = 10^5$ walkers by our random motion simulation technique. For programming in Matlab, Lorentz volume averaging was used, where the position of the circular section is considered fixed, while the initial position of the walker is considered random, within the section. Recall that the consecutive absolute positions $\boldsymbol{r}_i$ are dummy except that they define the construction steps $R_i = |\boldsymbol{r}_{i+1} - \boldsymbol{r}_i|$. To ensure uniform filling of the section required for volume averaging, it is sufficient to define the first radius R_1 directly by line code, $R(:,1) = R0 * (1 - sqrt(rand(N,1)))$, where N is the number of constructs and $R0$ is the pore radius. Constructions reach the limit relatively quickly, most often no more than thirty steps. By systematically taking 100 steps in one construction (without testing the final radius) we are almost sure of the success of the operation. Obviously the conception of Gibbs averaging can be used equivalently, by systematically starting the path construction at the origin and suitably distributing on one axis the distance of the disk region center to the origin, to simulate random positions in 2D space.

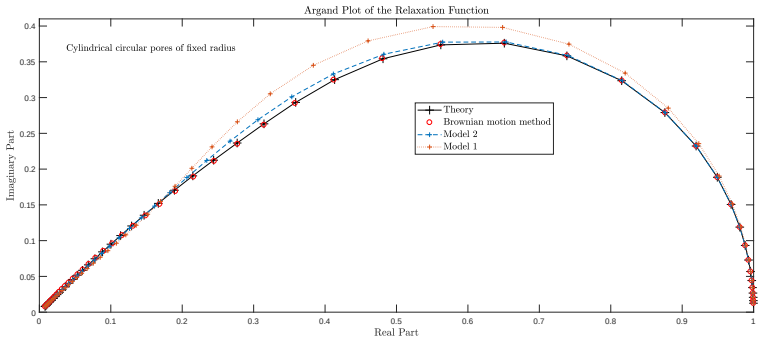

Fig. 2 Relaxation Function of cylindrical circular tubes: Theory, Random motion simulation, and Modeling.

All calculations were performed for 51 reduced frequencies, spanning the low, intermediate, and high frequencies. With $N = 10^5$ walkers as given on Fig. 2, the eye easily see that in the transition region, some of the black cross points indicating the theoretical values, are still not centred in the red circle points, that indicate the radioactive decay Brownian motion simulation. With $N = 10^7$ walkers not shown, the eye no longer perceives the differences. By the way with $N = 10^7$ walkers, the Eqs. (84) and (85) were found to give respectively the value, $0.1249996R^2$, for the parameter $k'_0 = k_0$, whose

theoretical value is, $R^2/8 = 0.125R^2$, and the value, 1.3336, for the parameter $\alpha'_0 = \alpha_0$, whose theoretical value is, $4/3 = 1.33333....$

Also plotted on the Figure 2, are the values (for the present case) of the following two general models.

Model 1 was derived by Lafarge [11], [2], in clarification of previous work by Allard and Champoux [12]. It is the thermal counterpart of Johnson et al. model [6] of the viscous dynamic tortuosity-permeability. For the effective bulk modulus it reads :

$$\frac{K_a}{K_f(\omega)} = \gamma - (\gamma - 1)\left[1 + \frac{\nu'\phi}{-i\omega k'_0}\left(1 - \frac{4i\omega k'^2_0}{\nu'\Lambda'^2\phi^2}\right)^{1/2}\right]^{-1}. \tag{103}$$

In general, the thermal permeability k'_0 and thermal characteristic length Λ' are independent parameters. However, the following dimensionless ratio

$$M' = \frac{8k'_0}{\phi\Lambda'^2}, \tag{104}$$

is generally found to depart from unity by less than one order of magnitude. For the circular tubes here, M is equal to one as it is known results that $k'_0 = R^2/8\phi$ and $\Lambda' = R$, and the above expression simplifies and happens to coincide with the so-called Allard-Champoux simpler model :

$$\frac{K_a}{K_f(\omega)} = \gamma - (\gamma - 1)\left[1 + \frac{8\nu'}{-i\omega\Lambda'^2}\left(1 - \frac{i\omega\Lambda'^2}{16\nu'}\right)^{1/2}\right]^{-1}. \tag{105}$$

Thus here, Model 1 is not different from the usual widely used Allard-Champoux model that considers that, $k'_0 = \phi\Lambda'^2/8$. Making apparent the ratio M' in (103) it can be seen that the magnitude of k'_0, or Λ'^2, determines a rollover frequency where a transition occurs between low- and high-frequencies. The shape of this transition is affected by the value of the "form factor" M'.

Model 2 is a refined model also derived by Lafarge [11], [3], in clarification of previous work by Pride et al. [37]. It gives a better definition of the shape of the transition frequency region, by adding the information provided by the thermal static tortuosity parameter α'_0, which determines an additional form factor,

$$m' = \frac{M'}{4(\alpha'_0 - 1)}. \tag{106}$$

The refined model replaces the square root in (103) by the expression

$$1 - m' + m'\left(1 + \frac{M'}{2m'^2}\frac{-i\omega}{\nu'}\frac{k'_0}{\phi}\right)^{1/2}. \tag{107}$$

In doing so it is capable to retrieve the exact two first terms in (83). For an understanding of these models we refer to [6], [], [2], and [3] Appendix.

As we can see, Model 2 performs better than Model 1, however, small discrepancies subsist. The discrepancies are magnified in the Argand Plot representation, which particularly emphasizes the transition region. A direct look at the quantity of interest, the effective dynamic apparent modulus as a function of frequency, is given in Figures 3 and 4 where we plot the real and imaginary parts of the normalized bulk modulus versus reduced frequency $\Omega = \omega \Lambda'^2/8\nu'$. (This choice of the reduced frequency is because of the next illustration, see below). The number of walkers is 10^7 and the Brownian motion simulation cannot be distinguished from the theoretical values.

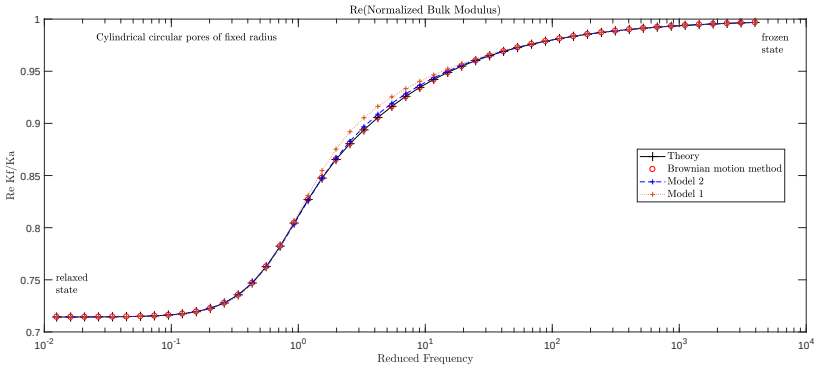

Fig. 3 Real part of $K_f(\omega)$ versus Reduced frequency $\Omega = \omega R^2/8\nu'$: Theory, Random motion simulation, and Modeling.

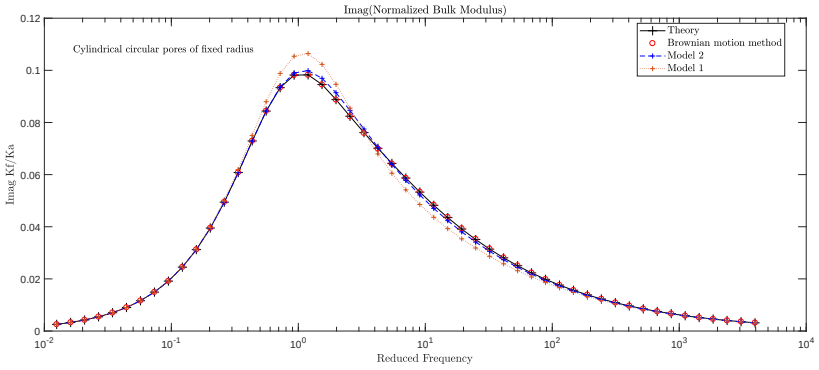

Fig. 4 Imaginary part of $K_f(\omega)$ versus Reduced frequency $\Omega = \omega R^2/8\nu'$: Theory, Random motion simulation, and Modeling.

What we can conclude from these figures and the numerical findings on k_0' and α_0' is that the Brownian motion method is validated. When the number of random walkers is not too high, it is possible to have very fast but not very precise estimates.

We now further illustrate the proposed algorithm by calculating the dynamic bulk modulus of air in two different $2D$ arrays of fibers surrounded by air (see Figure 5): a regular square array and a "random" array, both at porosity $\phi = 0.97$. We put random into quotes because the fibers positions were not completely random as the fibers were impenetrable. As illustrated on the Figure 5, we based our random geometry on a region of dimension $21L \times 21L$ in which 441 fibers of radius $R_0 = L\sqrt{(1-\phi)/\pi}$ were accomodated. We now further illustrate the proposed algorithm by calculating the dynamic bulk modulus of air in two different $2D$ fiber arrays surrounded by air (see Figure 5): a regular square array and a "random" array, both at porosity $\phi = 0.97$. We put random into quotes because the fiber positions are not completely random since the fibers are not penetrable. As illustrated in Figure 5, we based our random geometry on a $21L$ by $21L$ square region in which 441 fibers with radius $R_0 = L\sqrt{(1-\phi)/\pi}$ are accommodated.

The 441 fibers were successively randomly introduced in the region. When a fiber overlapped a preceding one, or when it overlapped the origin of the walkers random motion, (central position of the region), and origin of the construction of the ray suite, $[R_1, R_2, ..., R_n, ...]$, the position was rejected. A new random position was selected, and so on. In the regular case, to save time, we adapt the same general programming scheme, using 441 regularly spaced fibers but performing Gibbs random positioning of the whole configuration around the origin, avoiding overlap with the central fiber.

In both geometries the paths $[\boldsymbol{r}_1, \boldsymbol{r}_2, ..., \boldsymbol{r}_n, ...]$ were found to never go outside the $21L$ by $21L$ region, with typical drift, before reaching the pore walls, observed to be on the order of L. Very rarely, a drift as large as $8L$ was observed in the random geometry. Note that the drift values give an idea of the representative cell dimensions of the material's microstructure.

Note also that, by eliminating the overlap between fibers, we automatically ensure that the porosity ϕ and the thermal characteristic length Λ' in both geometries, random and regular, are the same, (Λ' is here automatically $R\phi/(1-\phi)$). Thus, using the reduced frequency, $\Omega = \omega\Lambda'^2/8/8\nu'$, we know that we should get the exact same frequency dependence for both geometries in the HF asymptotic limit. All calculations are done for the same 51 reduced frequencies as before.

It will be shown in this illustration that the irregular position of the fibers in real glass wool has a direct influence on the thermal relaxation of the effective bulk modulus, i.e. the way of moving from a relaxed isothermal state to a frozen adiabatic state. Note that due to the large density of glass compared to air, a porosity as high as $\phi = 0.97$ is still a safe value to ensure that the fibers essentially remain at ambient temperature, justifying the assumed boundary conditions (28).

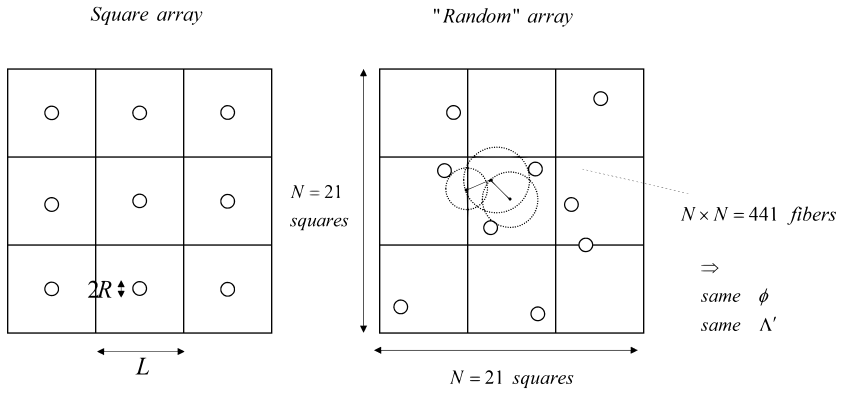

Fig. 5 The two different regular and "random" arrangements of cylinders. In the "random" case, $N = 21$, there are 441 fibers in our representative cell. Each walker is released at the origin, where no fiber is present, and see a new configuration. 10^7 walkers have been taken. In the regular arrangement each walker is released at random position in the central square in the fluid.

The real part of the dynamic bulk modulus for the regular and "random" settings at porosity $\phi = 0.97$ is plotted in Fig. 6 versus the reduced frequency, $\Omega = \omega \Lambda'^2/8\nu'$. The corresponding imaginary part is plotted in Fig. 7. The predictions of Model 1 and Model 2 are also indicated, using as input parameters for k_0' and α_0' the values inferred from the random walk algorithm, that were calculated beforehand using (84) and (85).

We note that we dispose of prior determinations of the parameters k_0' and α_0 in Cortis Ph.D. thesis [39] for the regular square setting at porosity $\phi = 0.97$. They were made by using FreeFM finite elements. Here, with $N = 10^7$ random walkers and by systematically taking 150 steps for one construction, (rare events were observed where the previous value 100 was insufficient to reach the boundary), our values are $k_0'/\phi = 0.17141L^2$ and $\alpha_0' = 1.0660$. Those of Cortis were $k_0'/\phi = 0.17144L^2$ and $\alpha_0' = 1.0654$. The differences concern digits that are not significant.

In the random case the value of the static thermal permability is found to be approximately two times (1.87) that of the regular arrangement (namely $0.3197L^2$ versus $0.1714L^2$). Thus the transition frequency is shifted to lower frequencies. The transition is steeper in the regular case, corresponding to a geometry where microscopic scales are less distributed than in the random case. This effect is better described by an enhanced model where a second form factor (106) allows accounting for the expansion of the transition. Indeed, it can be noted that the value of the thermal tortuosity α_0' which is a measure of disorder in the relaxed excess-temperature pattern, increases significantly in the random case (1.3833 versus 1.0660), leading to a rather small value of the shape factor m' (0.1671 versus 0.5205). This is why model 1, which assumes $m' = 1$, is significantly less precise in the random case. Model 2

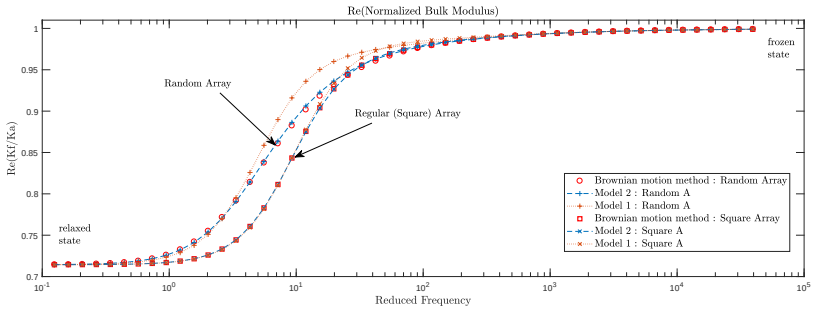

Fig. 6 Real part of the normalized bulk modulus $K_f(\omega)/K_a$ versus reduced frequency $\Omega = \omega\Lambda'^2/8\nu'$ for the two different regular and "random" arrangements of cylinders.

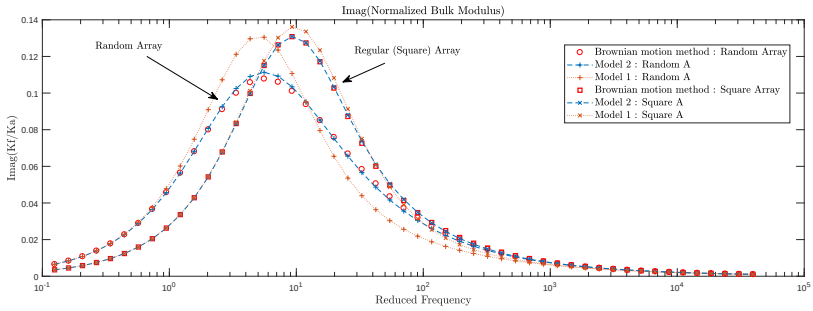

Fig. 7 Imaginary part of the normalized bulk modulus $K_f(\omega)/K_a$ versus reduced frequency $\Omega = \omega\Lambda'^2/8\nu'$ for the two different regular and "random" arrangements of cylinders.

is also less precise, but to a much lesser extent. Clearly, the proposed random walk method provides an efficient way to numerically calculate quasi-exactly the dynamic bulk modulus in a given geometry.

7 Conclusion

A very simple simulation technique utilizing the known properties of Brownian motion with radioactive decay has been proposed to estimate the dynamic bulk modulus of a gas filling a porous medium. This technique has been validated on the simplest case of a cylindrical circular tube, and shown to provide a convenient way to calculate thermal relaxation in arbitrary geometries. One useful characteristic of this method is its ability to obtain results in parallel for all frequencies of interest.

The case of regular and random parallel fiber arrangement is considered because it corresponds to two extreme cases of glass wool microgeometry. The results of the quasi exact Brownian motion determination of the relaxation pattern of the function $K_f(\omega)$ are in good agreement with the simple relaxation function proposed in the past (Lafarge, 1993) in terms of the following pore space geometric parameters: porosity ϕ, static permeability k_0', thermal tortuosity α_0', and thermal characteristic length Λ'. They also showed that the proper fiber arrangement has a significant influence on the shape of the relaxation transition.

The proposed simulation technique can provide useful clues on the underlying questions relative to the notion of macroscopic averaging. It is easy to implement and can be directly applied to all problems related to diffusion-controlled reactions between sinks, where the diffusing species are added in volume by using a spatially uniform time-harmonic source.

In forthcoming work we will show the power of this mesh-free method by quickly obtaining the thermal functions in pores with fractal boundary.

References

1. J.F. Allard and N. Atalla, Propagation of Sound in Porous Media: Modelling Sound Absorbing Materials, 2nd Edition, Wiley-Blackwell, Hoboken, 2009.
2. D. Lafarge, P. Lemarinier, J.F. Allard, and V. Tarnow, Dynamic compressibility of air in porous structures at audible frequencies, J. Acoust. Soc. Am. **102**, 1995 (1997).
3. D. Lafarge, Nonlocal Dynamic Homogenization of Fluid-Saturated Metamaterials. In: Jimnez, N., Umnova, O., Groby, JP. (eds) Acoustic Waves in Periodic Structures, Metamaterials, and Porous Media. Topics in Applied Physics, vol 143. Springer, Cham, (2021). doi: $10.1007/978-3-030-84300-7_7$
4. D. Lafarge, Acoustic Wave Propagation in Viscothermal Fluids. In: Jimnez, N., Umnova, O., Groby, JP. (eds) Acoustic Waves in Periodic Structures, Metamaterials, and Porous Media. Topics in Applied Physics, vol 143. Springer, Cham (2021). doi: $10.1007/978-3-030-84300-7_6$
5. A.D. Pierce, *Acoustics: An Introduction to Its Physical Principles and Applications*, Acoustical Society of America, 1989.
6. D.L. Johnson, J. Koplik, and D. Dashen, Theory of dynamic permeability and tortuosity in fluid-saturated porous media, J. Fluid Mech. **176**, 379 (1987).
7. L.L. Beranek, Acoustic impedance of porous materials, J. Acoust.Soc. Am. **13**, 248260 (1942).
8. S. Torquato and I.C. Kim, Efficient simulation technique to compute effective properties of heterogeneous media, Appl. Phys. Lett. **55**, 1847 (1989); https://doi.org/10.1063/1.102184
9. D. Lafarge, Determination of the dynamic bulk modulus of gases saturating porous media by Brownian motion simulation, in *Poromechanics II.* Proceedings of the Second Biot Conference on Poromechanics, edited by J.L. Auriault (Swets & Zeitlinger, Grenoble, 2002), pp. 703-708.
10. S. Lifson and J. Jackson, On the SelfDiffusion of Ions in a Polyelectrolyte Solution, J. Chem. Phys. **36**, 2410 (1962); doi: 10.1063/1.1732899

11. D. Lafarge, *Propagation du son dans les matériaux poreux à structure rigide saturés par un fluide viscothermique*, Université du Maine, Le Mans, (1993), http://www.theses.fr/1993LEMA1009
12. Y. Champoux and J.F. Allard, Dynamic tortuosity and bulk modulus in air-saturated porous media, J. Appl. Phys. **70** (4), 19751979 (1991).
13. M.A. Biot, The theory of propagation of elastic waves in a fluid-saturated porous solid, I. Low-frequency range, II. Higher frequency range, J. Acoust. Soc. Am. **28**, 168-191 (1956).
14. T.J. Plona, Observation of a second bulk compressional wave in a porous medium at ultrasonic frequencies, Appl. Phys. Lett. **36**, 259 (1980).
15. D.L. Johnson, Equivalence between fourth sound in liquid HeII at low temperatures and the Biot slow wave in consolidated porous media, Appl. Phys. Lett. **37**, 1065 (1980); Erratum: Equivalence between fourth sound in liquid Heii at low temperatures and the Biot slow wave in consolidated porous media, ibid **38**, 827 (1980) (E).
16. R. Burridge and J.B. Keller, Poroelastisity Equations Derived from Microstructure, J. Acoust. Soc. Am. **70**, 1140 (1981).
17. J.F. Allard, Y. Champoux, and C. Depollier, Modelization of layered sound absorbing materials with transfer matrices, J. Acoust. Soc. Amer. **82**, 17926 (1987).
18. C. Depollier, J.F. Allard and W. Lauriks, Biot theory and stressstrain equations in porous sound absorbing materials, J. Acoust. Soc. Amer. **84**, 22779 (1988).
19. W. Lauriks, A. Cops, J.F. Allard, C. Depollier and P. Rebillard, Modelization at oblique incidence of layered porous materials with impervious screens, J. Acoust. Soc. Amer. **87**, 12006 (1990).
20. J.F. Allard, C. Depollier, P. Guignouard and P. Rebillard, Effect of a resonance of the frame on the surface impedance of glass wool of high density and stiffness, J. Acoust. Soc. Amer. **89**, 9991001 (1991).
21. P. Guignouard, M. Meisser, J.F. Allard, P. Rebillard and C. Depollier, Prediction and measurement of the acoustical impedance and absorption coefficient at oblique incidence of porous layers with perforated facings, Noise Control Eng. J . **36**, 12935 (1991).
22. J.S. Bolton, N.M. Shiau and Y.J. Kang, Sound transmission through multi-panel structures lined with elastic porous materials, J. Sound Vib. **191**, 317-47 (1996).
23. D.L. Johnson and T.J. Plona, Recent developments in the acoustic properties of porous media, in Proceedings of the International School of Physics Enrico Fermi, Course XCIII, edited by D. Sette (North Holland, Amsterdam, 1986), pp. 255290.
24. M.A. Biot and D.G. Willis, The elastic coefficients of the theory of consolidation, J. Appl. Mech. **24** (4), 594-601 (1957).
25. A.N. Norris, On the viscodynamic operator in Biots equations of poroelasticity, J. Wave Mat. Interact. **1**, 365380 (1986).
26. L.D. Landau and E. Lifshitz, *Fluid Mechanics*, Pergamon Press, 1987.
27. E. Sanchez-Palencia, *Non-Homogeneous Media and Vibration Theory*, Lecture Notes in Physics, Volume 127 Springer-Verlag, 1980.
28. C. Boutin and C. Geindreau, Estimates and bounds of dynamic permeability of granular media, Journal Acoust. Soc. Am. **124**, 3576 (2009).
29. M. Avellaneda and S. Torquato, Rigorous link between fluid permeability, electrical conductivity, and relaxation times for transport in porous media, Phys. Fluids A **3**, 2529 (1991).
30. T. Levy and E. Sanchez-Palencia, Equations and interface conditions for acoustic phenomena in porous media, J. Math. Anal. And Appl. **61** 813-834 (1977).
31. L. Pontrjagin, A. Andronow, and A. Witt, Soviet Phys. – JETP **3**, 172 (1933).
32. C. Perrot, R. Panneton, X. Olny, Computation of the dynamic thermal dissipation properties of porous media by Brownian motion simulation: Application to an open-cell aluminum foam, J. Appl. Phys. **102**, 074917 (2007); doi: 10.1063/1.2786899

33. L.H. Zheng and Y.C. Chiew, Computer simulation of diffusioncontrolled reactions in dispersions of spherical sinks, J. Chem. Phys. **90**, 322 (1989).
34. G. Klein, Mean first-passage times of Brownian motion and related problems, Proc. Roy. Soc. (London) **A2ll**, 431 (1952).
35. C. Zwikker and C.W. Kosten, Sound absorbing materials, Elsevier Publishing company, Inc., New York, 1949, Reprinted 2012 by the NAG (Nederlands Akoestisch Genootschap).
36. R. Roncen, Z.E.A. Fellah, D. Lafarge, E. Piot, F. Simon, E. Ogam, M. Fellah and C. Depollier, Acoustical Modeling and Bayesian Inference for Rigid Porous Media in the Low- Mid Frequency Regime, J. Acoust. Soc. Am. 144, 3084 (2018).
37. S.R. Pride, F.D. Morgan, A.F. Gangi, Drag forces of porous-medium acoustics, Phys. Rev. B **47** 4964-4978 (1993).
38. D. Smeulders, R. Eggels and M. Van Dongen, Dynamic permeability: reformulation of theory and new experimental data, J. Fluid Mech. 245, 211 227 (1992).
39. A. Cortis, *Dynamic acoustic parameters of porous media: A theoretical, numerical and experimental investigation*, 2002-05-07, Civil Engineering and Geosciences, Delft University Press, ISBN 90-407-2294-3.